ISSN 2220-315x (online)

World Journal of *Experimental Medicine*

World J Exp Med 2020 January 8; 10(1): 1-9



Published by Baishideng Publishing Group Inc

World Journal of Experimental Medicine

Contents

Irregular Volume 10 Number 1 January 8, 2020

ORIGINAL ARTICLE

Basic Study

1 Alendronate disturbs femoral growth due to changes during immunolocalization of transforming growth factor-β1 and bone morphogenetic protein-2 in epiphyseal plate
Vieira JS, Cunha EJ, de Souza JF, Chaves LHK, de Souza JL, Giovanini AF

Contents

World Journal of Experimental Medicine

Volume 10 Number 1 January 8, 2020

ABOUT COVER

Editorial Board Member of *World Journal of Experimental Medicine*, Kwon-Soo Ha, PhD, Professor, Department of Molecular & Cellular Biochemistry, Kangwon National University School of Medicine, Chuncheon 24341, South Korea

AIMS AND SCOPE

The primary aim of the *World Journal of Experimental Medicine* (*WJEM*, *World J Exp Med*) is to provide scholars and readers from various fields of experimental medicine with a platform to publish high-quality basic and clinical research articles and communicate their research findings online.

WJEM mainly publishes articles reporting research results and findings obtained in the field of experimental medicine and covering a wide range of topics including clinical laboratory medicine (applied and basic research in hematology, body fluid examination, cytomorphology, genetic diagnosis of hematological disorders, thrombosis and hemostasis, and blood typing and transfusion), biochemical examination (applied and basic research in laboratory automation and information system, biochemical methodology, and biochemical diagnostics), *etc*.

INDEXING/ABSTRACTING

The *WJEM* is now abstracted and indexed in PubMed, PubMed Central, China National Knowledge Infrastructure (CNKI), and Superstar Journals Database.

RESPONSIBLE EDITORS FOR THIS ISSUE

Responsible Electronic Editor: *Yun-Xiaojian Wu*

Proofing Production Department Director: *Xiang Li*

NAME OF JOURNAL
World Journal of Experimental Medicine

ISSN
ISSN 2220-315x (online)

LAUNCH DATE
December 20, 2011

FREQUENCY
Irregular

EDITORS-IN-CHIEF
Arnon Blum

EDITORIAL BOARD MEMBERS
https://www.wjgnet.com/2220-315x/editorialboard.htm

EDITORIAL OFFICE
Jia-Ping Yan, Director

PUBLICATION DATE
January 8, 2020

COPYRIGHT
© 2020 Baishideng Publishing Group Inc

INSTRUCTIONS TO AUTHORS
https://www.wjgnet.com/bpg/gerinfo/204

GUIDELINES FOR ETHICS DOCUMENTS
https://www.wjgnet.com/bpg/GerInfo/287

GUIDELINES FOR NON-NATIVE SPEAKERS OF ENGLISH
https://www.wjgnet.com/bpg/gerinfo/240

PUBLICATION MISCONDUCT
https://www.wjgnet.com/bpg/gerinfo/208

ARTICLE PROCESSING CHARGE
https://www.wjgnet.com/bpg/gerinfo/242

STEPS FOR SUBMITTING MANUSCRIPTS
https://www.wjgnet.com/bpg/GerInfo/239

ONLINE SUBMISSION
https://www.f6publishing.com

© 2020 Baishideng Publishing Group Inc. All rights reserved. 7041 Koll Center Parkway, Suite 160, Pleasanton, CA 94566, USA
E-mail: bpgoffice@wjgnet.com https://www.wjgnet.com

World Journal of Experimental Medicine

Submit a Manuscript: https://www.f6publishing.com

World J Exp Med 2020 January 8; 10(1): 1-9

DOI: 10.5493/wjem.v10.i1.1

ISSN 2220-315x (online)

ORIGINAL ARTICLE

Basic Study

Alendronate disturbs femoral growth due to changes during immunolocalization of transforming growth factor-β1 and bone morphogenetic protein-2 in epiphyseal plate

Juliana Souza Vieira, Emanuelle Juliana Cunha, Juliana Feltrin de Souza, Luis Henrique Koeler Chaves, Jessica Lakes de Souza, Allan Fernando Giovanini

ORCID number: Juliana Souza Vieira (0000-0001-6297-5784); Emanuelle Juliana Cunha (0000-0002-6780-7904); Juliana Feltrin de Souza (0000-0001-9969-3721); Luis Henrique Koeler Chaves (0000-0002-8463-7361); Jessica Lakes de Souza (0000-0003-2840-5811); Allan Fernando Giovanini (0000-0002-1637-2955).

Author contributions: Vieira JS and Cunha EJ performed equally the majority of laboratorial experiments; de Souza JF, Chaves LHK and de Souza JL participated in treatment of animals and performed the immunohistochemical investigations; Giovanini AF analyzed all data and wrote the paper.

Institutional animal care and use committee statement: The principles of laboratory animal care and national laws on animal use were observed for the present study with the approval of the Ethical Committee for Animal Research of Positive University (Protocol #266).

Conflict-of-interest statement: Nothing to disclose.

Data sharing statement: No additional data are available.

ARRIVE guidelines statement: The authors have read the ARRIVE guidelines, and the manuscript was prepared and revised

Juliana Souza Vieira, Emanuelle Juliana Cunha, Luis Henrique Koeler Chaves, Jessica Lakes de Souza, Allan Fernando Giovanini, Clinical Dentistry, University Positivo, Curitiba, PR 81280-330, Brazil

Juliana Feltrin de Souza, Stomatology Department, University Federal of Paraná, Curitiba, PR 80210-170, Brazil

Corresponding author: Allan Fernando Giovanini, MD, PhD, Associate Professor, Clinical Dentistry, University Positivo, R Pedro Viriato Parigot de Souza, 5300 Campo Comprido, Curitiba, PR 81280-330, Brazil. afgiovanini@gmail.com

Abstract

BACKGROUND

The epiphyseal growth plate is an important anatomical segment localized on the ends of a long bone. Despite the abovementioned atractive reasons for alendronate's use, few data on the effect of alendronate during epiphyseal growth exist.

AIM

Verify the effect of alendronate on the growth epiphyseal plate, and compare its effect with the size of the femur during the double-staining of the immunolocalization of transforming growth factor-β1 (TGF-β1) and bone morphogenetic protein-2 (BMP2) in endochondral ossifing in specimens that have received alendronate.

METHODS

Forty newborn rats were randomly divided into two groups: a control group (were given applications of 1 mg/kg physiologic saline) and a group that received Alendronate (a dose of 2.5 mg/kg). These groups were then divided into two subgroups for euthanasia in two and 12 d of life. After euthanasia, the femurs were removed, and the femoral bones were measured linearly between the apex of the greater trochanter until the lower intercondylar midlle face to verify the probable bone growth between 3 and 12 d in control and aledroanto treated rats. Posteriorly, the surgical pieces were also sent to the histopathology laboratory to produce histological slides. The obtained slides were stained with hematoxylin and eosin to measure each of the cartilage zones in endochondral development. and other slides were immunohistochemically tested for anti- TGF-

according to the ARRIVE guidelines.

Open-Access: This article is an open-access article which was selected by an in-house editor and fully peer-reviewed by external reviewers. It is distributed in accordance with the Creative Commons Attribution Non Commercial (CC BY-NC 4.0) license, which permits others to distribute, remix, adapt, build upon this work non-commercially, and license their derivative works on different terms, provided the original work is properly cited and the use is non-commercial. See: http://creativecommons.org/licenses/by-nc/4.0/

Manuscript source: Unsolicited manuscript

Received: May 6, 2019
Peer-review started: May 6, 2019
First decision: September 2, 2019
Revised: November 26, 2019
Accepted: December 14, 2019
Article in press: December 14, 2019
Published online: January 8, 2020

P-Reviewer: Stavroulopoulos A
S-Editor: Ma RY
L-Editor: A
E-Editor: Wu YXJ

β1 and BMP-2 antibodies to investigate the immunolocalization of these proteins in the epiphyseal plaque area.

RESULTS

On the third day, some diferences between the control group and specimens treated with alendronate were verified. Macroscopiccaly, we found similarities in size between the femoral bones when we compared the control group with the specimens that received alendronate. On the 12th day, the bone size of the mice receiving the drug was significantly smaller than those of the control group. These results coincide with changes in the TGF-β1 and BMP-2 expression. In the specimens that received alendronate, the TGF-β1 was expressed in some sites of trabecular bone that was neoformed, peripherally to the bone marrow area. The BMP-2 was also positive in proliferative chondrocytes and hypertrofic chondrocytes. On the 12th day, all layers of chondrocytes exhibited positivity for BMP-2 in the specimens that received alendronate. In the interface between the trabecular bone and cartilage, an area of disorganized bone deposition was evident. Neoformed bone also appeared to be different at 12 d. In the control group, BMP-2 was positive in an intense area of bone trabeculae, whereas the alendronate-treated group showed TGF-β1 positive trabeculae and a greater bone area.

CONCLUSION

Alendronate alters the immunolocalization of TGF-β1 and BMP-2 simultaneously, a condition that changes the usual histological aspects of the cartilage zone and impairs epiphysis growth and femur growth.

Key words: Alendronate; Bone development; Epiphyseal plate; Bone morphogentic protein-2; Transforming growth factor-β1

©The Author(s) 2020. Published by Baishideng Publishing Group Inc. All rights reserved.

Core tip: This is the first study that addresses the likely action of alendronate in appendicular bone development. Through of macroscopic, immunohistochemical and histological analysis, we revealed that alendronatemay impairs the bone growth, since alters the usual development of epiphyseal plate associated to changes in the immunolocalization of transforming growth factor-β1 and bone morphogenetic protein-2.

Citation: Vieira JS, Cunha EJ, de Souza JF, Chaves LHK, de Souza JL, Giovanini AF. Alendronate disturbs femoral growth due to changes during immunolocalization of transforming growth factor-β1 and bone morphogenetic protein-2 in epiphyseal plate. *World J Exp Med* 2020; 10(1): 1-9
URL: https://www.wjgnet.com/2220-315x/full/v10/i1/1.htm
DOI: https://dx.doi.org/10.5493/wjem.v10.i1.1

INTRODUCTION

The epiphyseal growth plate is an important anatomical segment localized on the ends of a long bone. It is responsible for the longitudinal growth of children's long bones through coordinated sequence changes to the cartilage histomorphological aspects. The zones encountered in the growth plate include the reserve, proliferative, maturation, and hypertrophy zones. The zone of hypertrophy[1] is where the substitution of a portion of cartilage in the osteoprogenitor cells takes place. This is where bone matrix deposition appears posteriorly[2].

This well-orchestrated histomorphological transition for diverse chondroid aspects takes place until effective endochondral ossification occurs, and it seems to be regulated through autocrine and paracrine stimulation. An important growth factor that operates during stages of chondroid modification and endochondral ossification is the transforming growth factor-β1 (TGF-β1).

Supporting this context, the TGF-β1 works to maintain the reserve of chondrocyte

clones, inhibits premature terminal hypertrophic differentiation in pre-hypertrophic chondrocytes[3], arrests differentiation at an early stage of hypertrophy, and induces the coexistence of bone proteins that culminates in an osteoblastic appearance[4].

For osteoblast differentiation, the induction of bone morphogenetic protein-2 (BMP2) expression through TGF-β1[5] in hypertrophic chondrocytes appears to be crucial. BMP-2 directs mesenchymal cells to the osteoblast lineage, triggers the expression of major bone matrix protein genes, and orchestrates the production of phosphatase alkaline to mineralize the matrix so as to form bone[6].

Given the important roles of TGF-β1 in chondrogenesis and osteogenesis, a lack of transcription in this cytokine invariably leads to skeletal disorders and developmental defects in children-for example, fibrodysplasia ossificans progressiva[7], Camurati-Engelmann disease[8], and brachydactyly, especially type A2[9].

Thus, pharmacological agents that may stimulate a source of TGF-β1 at the same time, which may contribute to chondroprotection and modulate bone formation, are widely required for treatments for children[10-12]. It is established in the literature that the prolonged administration of alendronate, which is a nitrogenous bisphosphonate, may improve and mantain for a higher period of time the expression of TGF-β1 on an organism[12]. On other hand, the use of this drug has also been used to protect the bone tissue against the hyperactivity of osteoclasts or the bone metastasis of several neoplasms.

Despite the abovementioned atractive reasons for alendronate's use, few data on the effect of alendronate during epiphyseal growth exist. Thus, the aim of this study was to verify the histological response of the epiphyseal growth plate under the action of alendronate in newborn rats and to compare these results with that of double-staining the immunolocalization of TGF-β1 and BMP-2. We compare these histological and immunohistochemical aspects with the size of the femur.

MATERIALS AND METHODS

The principles of laboratory animal care and national laws on animal use were observed for the present study with the approval of the Ethical Committee for Animal Research of Positive University (Protocol #266).

Obtainig the speciemens

Seven two old months female rats (Rattus norvegicus albinus, Holtzman), weighing aproximately 250 g, were used as a progenitress source. The animals were maintained in a department with controlled temperature (22 ± 2 °C), humidity (55% ± 5%), with a 12h/12h light/dark cycle and food and water available ad libitum.

In this study, the species of neonatal rats were obtained from natural generation according to the study by de Souza *et al*[13].

A group of newborn rats received a sterile 0.9% saline solution (n = 20 – control group), whereas other newborn rats (n = 20) received 2.5 mg/kg per day of alendronate trihydrate (Biolife, Curitiba, Brazil, Lote: 14042132C) (alendronate group). All solutions (saline or drug) were administered intraperitorially daily up to the euthanasia time period, which occurred on the third and 12th days after the rat's birthday (n = 10 for group for each time period). All euthanasia was performed by using overdoses of isofluorane.

Macroscopic measurement of femur

After euthanasia, the legs of the newborn rats were immediately removed, and the femur was measured linearly between the apex of the greater trochanter and the lower intercondylar midface using a pachymeter. The values were tabulated and subjected to statistical analysis.

Processing of specimens for microscopic analysis

Following mensuration, each surgical piece obtained was immersed in a fixative solution for 48 h at room temperature in 4% formaldehyde that was buffered to pH 7.2 with 0.1 mol/L sodium phosphate and posteriorly immersed in 7% disodium ethylenediaminetetraacetic acid for decalcification for aproximately 2 wk. After decalcification each the specimens were dehydrated in ethanol, cleared in xilene, and embedded in paraffin.

From each specimen, serial 3-μm-thick fragments were obtained and adhered to slides. The sections were carefully formed in the longitudinal plane of the femoral bone in the anterior-posterior section. Some slides containing the fragments were stained with hematoxilin and eosin to verify the histological aspects of bone, whereas other sections of fragments were submitted for double immunohistochemical detection for anti-TGF-β1 and BMP-2.

Immunohistochemistry processing

From each specimen, sections 3 micrometers thick were submitted to the immunohistochemical detection of all proteins. For antigen retrieval, deparaffinized sections were immersed in 10 mmol/L sodium citrate buffer (pH 6.0) and subjected to a microwave three times for 5-min cycles. The sections were then incubated overnight at 4 °C with primary BMP-2 (0.5 mg/mL, ab6285; Abcam, Cambridge, United Kingdom) with a dilution factor of 1:150. The labeled akaline-phosphatasis antibody-binding detection system (Universal HRP immunostaining kit – Diagnostic Byosystem, Foster City, CA, United States) was employed to detect the primary antibodies for 30 min, whereas the revelation of the immunohistochemical reaction was performed with Fast Red substrate, producing a red color in positive protein sites. The specimens were washed in phosphate-buffeed saline (pH 7.2), the sections were incubated overnight at 4 °C with primary TGF-β1 (200 mg/mL, sc-146; Santa Cruz Biotechnology, Santa Cruz, CA, United States), with a dilution factor of 1:200. The labeled streptavidin biotin antibody-binding detection system (Universal HRP immunostaining kit – Diagnostic Byosystem, Foster City, CA, United States) was employed to detect the TGF-β1. Following washing in 0.05 mol/L Tris-HCl buffer (pH 7.2), the sections were incubated for 30 min at room temperature in biotinylated anti-rabbit/mouse/goat immunoglobulin (LSAB-plus Kit, Dako, CA, United States) and were revealed with diamine benzidine, producing a brownish color in the sites positive for protein. All of the sections were counterstained with Harris hematoxylin. For the negative control, the primary antibodies were omitted.

Analyses

Images of immunohistochemistry sections were taken with a digital camera (DP-71, Olympus, Tokyo, Japan) connected to a microscope (BX-51, Olympus, Tokyo, Japan), and DP Controller software (Version 2.1.1.183, Olympus, Tóquio, Japan) with an original magnification of × 100. The digital images were collected and saved with a resolution of 300 dpi (image size 113.66 cm × 75.95 cm). All histomorphometric measurements were made with Image J software. The data were counted manually. The perimeter of each morphological zone of endochondral ossifying was carefully drawn and measured, and they are presented in mm^2. The immunohistochemistry protein identified as a brown color for TGF-β1 or a red color for BMP-2 were manually counted and tagged. An image of a 1-mm slide micrometer was used to calibrate all measurements for areas, whereas positive cells for both proteins were transformed into a percentage. The slides were analyzed for each of the above parameters. An average of the three measurements for each parameter was then calculated for each specimen.

Statistical analysis

The linear measurement of the femur, the areas of histological chondroid zones, and percentages of immunohistochemical data for each zone were evaluated within the monitoring period. An analysis of variance and Shapiro-Wilk analysis were used to determine the normality, followed by the Kruskal-Wallis non-parametric test to verify significant differences among groups. A P value < 0.05 was considered to be statistically significant.

RESULTS

Femur size

On the third day of analysis, the median values of the specimens that received alendronate were slightly larger than the median values of the linear measures of the femurs of the control species. In contrast to the control species, the growth between three to 12 d of analysis was scarce in the group that received alendronate. Thus, on the 12th day of analysis, the measures of the femurs of the specimens that received the drug were significantly lower when compared with the alendronate-free specimens. All data are present in Table 1.

Histological and histomorphometric data

A brief description of the histologic features found among groups is described bellow while the histomorphometric parameters are summarized in Table 2 (P < 0.05).

On the third day (Figure 1A), it was possible to verify that the areas of the reserve, proliferative, and maturation zones were similar (Figure 1Aa and b), whereas the hypertrophic zone was significantly larger in terms of the number of specimens that received alendronate (Figure 1Ab). On the 12th day, the control group exhibited similar characteristics when compared with the third day (Figure 1Ba). In contrast, the

Table 1 Median, minimum and maximum values of linear value found between the apex of the greater trochanter until to the lower intercondylar midlle face

Day	Linear Size of Femur (cm)		*P* value
	Control	Alendronate	
3	5.93 (5.67 – 6.04)	6.85 (5.99 – 7.21)	$P = 0.062$
12	12.72 (11.67-13.52)	8.84 (8.43 – 9.08)	$P = 0.027$

For each same time period values $P > 0.05$ are statistically similar.

specimens that received alendronate demonstrated significantly fewer areas of maturation and hypertrophic zones. However, an unorganized bone matrix deposition was observed between the hypertrophic zone and cortical bone (Figure 1Bb).

Double-staining for TGF-β1 and BMP-2

On the third day, only TGF-β1 was observed in the maturation and hpertrophic zones in the control group. In these specimens, the BMP-2 was positive in bone matrix deposition. All zones of cartilage revealed positivity for BMP-2, whereas the TGF-β1 was present in some proliferative cells and in the majority of cells that compounded both the maturation and the hypertrophic zone. In addition, intense double positivity for TGF-β1 and BMP-2 was observed in the bone matrix. On the 12th day, the control group exhibited a similar immunohistochemical pattern; however, it was possible to verify positivity for BMP-2 in hypertrophic cartilage and the medullary bone matrix. The alednronate group displayed the presence of BMP-2 in cartilage and in the bone matrix. In the area of the unorganized matrix, the BMP-2 was prevalent, whereas in the larger medular bone matrix, both proteins were detected (Table 3).

DISCUSSION

The study demonstrated that alendronate decreased the longitudinal femur size from three to 12 d post the prolonged administration of alendronate, a situation that coincided with changes in the usual histological aspects of chondroid zones, especially in the maturation and hypertrophic strata, as well as changes in co-immunoexpression between TGF-β1 and BMP-2.

To understand the changes that occurred, one must comprehend the importance of the usual immunolocalization of each protein and the likely effect that each protein exerted in usual conditions of endochondral growth.

In hyaline cartilage, TGF-β1 presence is required for the homeostasis of this anatomical area, and this cytokine seems to play a fundamental role in the production and remodelation of the chondroid extracellular matrix.

However, the action of TGF-β1 for each stratum of cartilage of the methaphisyae of long bones seems to be distinct[14]. In this pathway, D'Angelo *et al*[15] (2001) indicated that maturing and hypertrophic chondrocytes produce and express active TGF-β1, and this cytokine operates in paracrine form in another layer of cartilage. In this way, TGF-β1 influences maturation, proliferation, and hypertrophy, whereas its presence inhibits the terminal differentiation of mature chondrocytes. This effect may help chondrocytes to remain in the pre-hypertrophic stage, thus inhibiting their terminal differentiation to hypertrophic chondrocytes.

It is noteworthy that TGF-β1 positively regulates the expression of specific cartilage proteins during re-differentiation; conversely, substantial evidence shows that chondrocyte exposure to TGF-β1 during the proliferative phase obstructs these cells' re-differentiation potential[14,16]. This condition may explain the positivity seen in the TGF-β1 prevalent in the prehypertrophic and hypertrophic zones of cartilage as seen in our control group on the third and 12th days of analysis, despite the fact that some hypertrophic chondrocytes during this period exhibited positivity for BMP-2, whereas in the precocious time period, BMP-2 was positive only in the bone matrix.

In contrast, for specimens that received alendronate, we observed TGF-β1 in all strata of chondrocytes, a fact that coincided with a significantly larger area of the hypertrophic zone on the 3rd day. Furthermore, the cells of all chondroid strata also exhibited concomitant expression with BMP-2. This peculiar situation coincided with an unorganized bone matrix formation between a thinner layer of hypertrophic chondrocytes and trabecular bone on the 12th day of analysis. These results suggest

Table 2 Median, minimum and maximum values of area in mm2 of each chondroid zone

Cartilage zone	Area accounted (mm^2)					
	3rd day			12th day		
	Control	Alendronate	*P* value	Control	Alendronate	*P* value
Reserve	6.12 (5.52-6.51)	5.63 (5.07-5.71)	$P = 0.061$	3.33 (3.22-3.51)	2.26 (2.11-2.29)	$P = 0.056$
Proliferative	4.02 (3.82-4.44)	4.12 (3.98-4.58)	$P = 0.071$	3.38 (3.35-3.43)	3.11 (3.05-3.26)	$P = 0.061$
Maturation	0.4 (0.32-0.46)	0.36 (0.29-0.40)	$P = 0.073$	0.27 (0.16-0.29)	0.04 (0.01-0.06)	$P = 0.002$
Hipertrophic	4.12 (3.66-4.31)	7.59 (7.31-7.77)	$P = 0.032$	4.02 (3.96-4.26)	2.17 (2.11-2.32)	$P < 0.0001$

For each same time period values $P < 0.05$ were considered statistically different.

that alendronate may promote the cartilage expansion of the maturated and hypertrophic chondroid zones only during the early stages of the administration of the drug. However, the concomitant expression between TGF-β1 and BMP-2 in areas of the chondroid zones featuring endochondral ossification also indicates the likely premature transdifferentiation from cells of chondroid lineage to osteoprogenitor cells, especially when these specimens were exposed to the drug for a prolonged period of time.

It is noteworthy that our result is not an isolated finding in the literature and that some evidence shows that alendronate possesses an important osteogenic capacity. Supporting this perspective, Wang *et al*[17] (2010) demonstrated that the administration of alendronate in animal models was responsible for the transcription of osteoprogenitor genes in medullar mesenchymal cells. They also added that osteogenic potential occurs because the alendronate stimulates the MAP kinases' pathways, which, in turn, may excite the expression of osteoproteins. These effects may indicate and explain the previous radiological results published by Silva *et al*[18] (2010), who demonstrated sclerotic metaphyseal lines in the long bones of young patients treated with alendronate. They may also indicate that the extended use of alendronate compromises the usual growth of children and its bone development.

Thus, alendronate impairs the epiphysis growth plate at the same time as the growth of the femur, as it simultaneously alters the immunolocalization of TGF-β1 and BMP-2, and it may produces a precocious transdifferentiation from chondroid cells to osteogenic cells-a condition that impairs the usual development and epiphyseal plate, thus impairing femoral growth.

However, it should be highlighted that this study has some limitations. Herein, we evaluated the macroscopic, histological and immunohistochemical aspects on 3rd and 12th day of development and none data may be stipulated in the intermediated stages of development of epiphyseal plate. The immunohistochemistry staining identifies proteins present either chondroid matrix or bone matrix, regardless of the time when they were expressed.

In addition, this study focused only on epiphyseal plate area and the present results may not be extrapolated to total appendicular as well as craniofacial bones[19]. However, this study may give an important information, and it may contribute to the discussion over the clinical use of alendronate in earlier stages of bone development.

Table 3 Percentage in median, minimum and maximum for transforming growth factor-β1 and bone morphogenetic protein-2 values in cells for chondroid zone

Chondroid layer	Day	TGF-b1		*P* value	BMP-2		*P* value
		Control	Alendronate		Control	Alendronate	
Reserve	3	-	-	-	-	12 (10-14)	$P < 0.001$
	12	-	-	-	-	34 (30-36)	$P < 0.001$
Proliferative	3	23.01 (19-26)	16.27 (14-19)	$P = 0.047$	-	72.21 (70-75)	$P < 0.001$
	12	19.12 (17-23)	2.33 (0-3)	$P < 0.001$	-	67.43 (66-69)	$P < 0.001$
Maturation	3	89.64 (85-93)	93.07 (91-94)	$P = 0.673$	-	88.61 (86-81)	$P < 0.001$
	12	83 (80-84)	1.06 (0-1)	$P < 0.001$	13 (12-15)	94.05 (92-98)	$P < 0.001$
Hipertrophic	3	96.35 (94-99)	97.66 (95-98)	$P = 0.772$	2 (2-3)	82.17 (80-85)	$P < 0.001$
	12	93.52 (92-95)	92.31 (90-93)	$P = 0.694$	42 (41-44)	93.00 (90-95)	$P = 0.027$

For each same time period values $P < 0.05$ were considered statistically different.

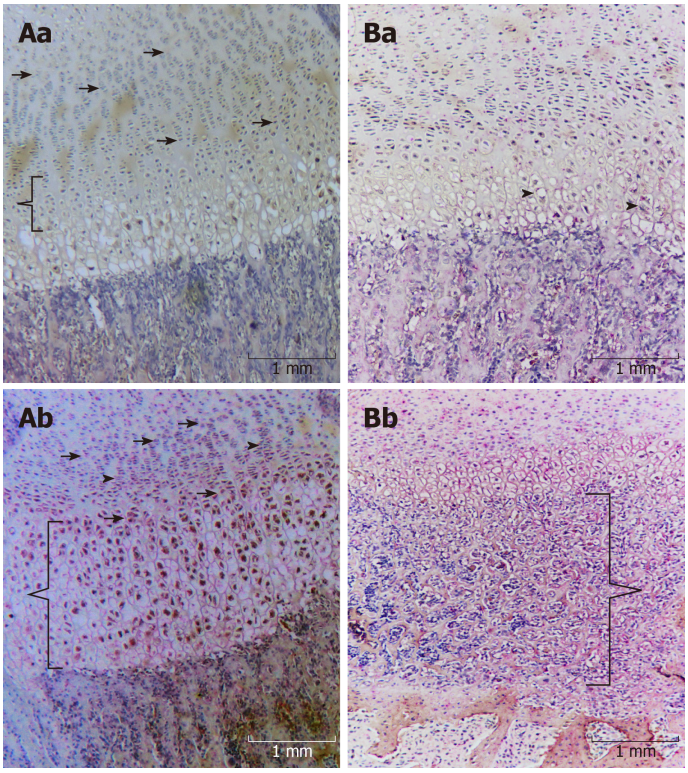


Figure 1 Histological and histomorphometric data. A: Endochondral ossification on 3rd day on control (a) and after Alendronate administration (b). Reveals positivity for transforming growth factor-β1 (TGF-β1) (brownish color) in proliferative (Chevron arrow), maturation (keys) and hyperplasic stratum of cartilage, while reserve stratum was negative. On other hand the group that received Alendronate there was an intense positivity for bone morphogenetic protein-2 (BMP2) (red color) in reserve stratum (arrow) and proliferative (head of arrow) zones, while maturation (chevron arrows) and hyperplasic stratum (brackets) of cartilage demonstated positivity for both TGF-β1 (brown) and BMP-2 (red). B: Endochondral ossification on 12th day. The micrographs (a) reveals the control group, and demonstrates similar pattern for TGF-β1, but also shows evident presence of BMP-2 in hyperplasic chondrocites (head of arrows). Micrograph (b) reveals the mantaining of presence of BMP-2 on all stratum of cartilage, at the same time that show an ectopic mineralization (brackets) and decrease of hypertrophic zone of chondrocytes with intense positivity for BMP-2.

ARTICLE HIGHLIGHTS

Research background

Endochondral ossifying constitutes the fundamental model for the development of appendicular skeletal formation. This process requires well-organized changes on the cartilage morphological aspects that includes the resting, proliferative, prehypertrophic, hypertrophic segments which it is followed by replacement of mineralized hypertrophic cartilage with osteoprogenitor cells, and the calcified cartilage is subsequently replaced by bone. Under pathological situation this usual development does not occur, promoting growth deficiencies. Since alendronate may contribute

either for chondrogenic or osteogenic development, herein we evaluated the likely effect of alendronate in epiphyseal plate of newborn rats, in order to verify the real effect of alendronate during earlier development of appendiclar bones.

Research motivation

The fundamental topics adressesd in the present study were: (1) Would be alendronate a drug that should be able to improve the chondrogenic and osteogenic in eralier stage of development; and (2) Alendronate alters the correlation between transforming growth factor-β1 (TGF-β1) and bone morphogenetic protein-2 (BMP2) during endochondral ossification? The answer of this question, could give us a direction between for a likely therapy apporach in child that possess congenital deficies of growth.

Research objectives

Thus, the main objective of this study was to verify how alendornate acts on the epifeaseal developmental plaque. In addition, we evaluated which region of endochondral development is most stimulated or inhibited by alendronate, as well as whether the drug may cause early ossification.

Research methods

Thus, we analyzed the evaluation of femoral bone growth of neonatal rats by measuring the distance between the apex of the greater trochanter until the lower intercondylar midlle face. We also measured the area of each stratification of the endochondral histological zones, as well as where the ossifications occurred - late or early. We also evaluated by immunohistochemistry, the immunopresence of TGF-β1 and BMP-2 in each of these endochondral zones.

Research results

Here we reveal that specimens given alednroanto developed greater cartilage hypertrophy while the reserve zone was decreasing. These results also coincide with changes in co-immunolocation between TGF-β1 and BMP-2. Here we demonstrate a greater presence of osteoprotein in areas where endochondral proliferation and endochondral diphonication should occur, triggering early ossification. These results also coincide with lower bone growth.

Research conclusions

In this study we may conclude that: (1) Alendronate may compromise the usual development and growth of epiphyseal plaque. (2) This pathological event may occur as alednronate provides prior expression of BMP-2, while TGF-1 immunolocation decreases. And (3) the fundamental result found here indicates that alendronate does not induce appendicular bone growth. Thus, it may indicate that the use of this drug is not a plausible conduct for children suffering from endochondral growth disorders.

Research perspectives

Here we suggest the perspective that alendronate compromises the development of long bones. There is a need for research using other drugs to try to promote greater growth of endochondral zones, ossification in suitable areas, conditions that are important for appendicular bone growth.

REFERENCES

1 **Emons J**, Chagin AS, Sävendahl L, Karperien M, Wit JM. Mechanisms of growth plate maturation and epiphyseal fusion. *Horm Res Paediatr* 2011; **75**: 383-391 [PMID: 21540578 DOI: 10.1159/000327788]

2 **Mackie EJ**, Ahmed YA, Tatarczuch L, Chen KS, Mirams M. Endochondral ossification: how cartilage is converted into bone in the developing skeleton. *Int J Biochem Cell Biol* 2008; **40**: 46-62 [PMID: 17659995 DOI: 10.1016/j.biocel.2007.06.009]

3 **Derynck R**, Akhurst RJ. Differentiation plasticity regulated by TGF-beta family proteins in development and disease. *Nat Cell Biol* 2007; **9**: 1000-1004 [PMID: 17762890 DOI: 10.1038/ncb434]

4 **Tekari A**, Luginbuehl R, Hofstetter W, Egli RJ. Transforming growth factor beta signaling is essential for the autonomous formation of cartilage-like tissue by expanded chondrocytes. *PLoS One* 2015; **10**: e0120857 [PMID: 25775021 DOI: 10.1371/journal.pone.0120857]

5 **Kang JS**, Alliston T, Delston R, Derynck R. Repression of Runx2 function by TGF-beta through recruitment of class II histone deacetylases by Smad3. *EMBO J* 2005; **24**: 2543-2555 [PMID: 15990875 DOI: 10.1038/sj.emboj.7600729]

6 **Harada S**, Rodan GA. Control of osteoblast function and regulation of bone mass. *Nature* 2003; **423**: 349-355 [PMID: 12748654 DOI: 10.1038/nature01660]

7 **Katagiri T**, Tsukamoto S, Nakachi Y, Kuratani M. Recent Topics in Fibrodysplasia Ossificans Progressiva. *Endocrinol Metab (Seoul)* 2018; **33**: 331-338 [PMID: 30229572 DOI: 10.3803/EnM.2018.33.3.331]

8 **Wang C**, Zhang BH, Liu YJ, Hu YQ, He JW, Zhang ZL. Transforming growth factor-β1 gene mutations and phenotypes in pediatric patients with CamuratiEngelmann disease. *Mol Med Rep* 2013; **7**: 1695-1699 [PMID: 23503840 DOI: 10.3892/mmr.2013.1367]

9 **Lehmann K**, Seemann P, Stricker S, Sammar M, Meyer B, Süring K, Majewski F, Tinschert S, Grzeschik KH, Müller D, Knaus P, Nürnberg P, Mundlos S. Mutations in bone morphogenetic protein receptor 1B cause brachydactyly type A2. *Proc Natl Acad Sci USA* 2003; **100**: 12277-12282 [PMID: 14523231 DOI: 10.1073/pnas.2133476100]

10 **Rahman MS**, Akhtar N, Jamil HM, Banik RS, Asaduzzaman SM. TGF-β/BMP signaling and other molecular events: regulation of osteoblastogenesis and bone formation. *Bone Res* 2015; **3**: 15005 [PMID: 26273537 DOI: 10.1038/boneres.2015.5]

11 **Cheung MS**. Drugs Used in Paediatric Bone and Calcium Disorders. *Endocr Dev* 2015; **28**: 277-290 [PMID: 26138848 DOI: 10.1159/000381053]

12 **Feehan AG**, Zacharin MR, Lim AS, Simm PJ. A comparative study of quality of life, functional and bone outcomes in osteogenesis imperfecta with bisphosphonate therapy initiated in childhood or adulthood. *Bone* 2018; **113**: 137-143 [PMID: 29787832 DOI: 10.1016/j.bone.2018.05.021]

13 **de Souza JF**, Gramasco M, Jeremias F, Santos-Pinto L, Giovanini AF, Cerri PS, Cordeiro Rde C. Amoxicillin diminishes the thickness of the enamel matrix that is deposited during the secretory stage in rats. *Int J Paediatr Dent* 2016; **26**: 199-210 [PMID: 26148818 DOI: 10.1111/ipd.12184]

14 **Li TF**, O'Keefe RJ, Chen D. TGF-beta signaling in chondrocytes. *Front Biosci* 2005; **10**: 681-688 [PMID: 15569609]

15 **Dangelo M**, Sarment DP, Billings PC, Pacifici M. Activation of transforming growth factor beta in chondrocytes undergoing endochondral ossification. *J Bone Miner Res* 2001; **16**: 2339-2347 [PMID: 11760850 DOI: 10.1359/jbmr.2001.16.12.2339]

16 **Narcisi R**, Quarto R, Ulivi V, Muraglia A, Molfetta L, Giannoni P. TGF β-1 administration during ex vivo expansion of human articular chondrocytes in a serum-free medium redirects the cell phenotype toward hypertrophy. *J Cell Physiol* 2012; **227**: 3282-3290 [PMID: 22105490 DOI: 10.1002/jcp.24024]

17 **Wang CZ**, Chen SM, Chen CH, Wang CK, Wang GJ, Chang JK, Ho ML. The effect of the local delivery of alendronate on human adipose-derived stem cell-based bone regeneration. *Biomaterials* 2010; **31**: 8674-8683 [PMID: 20719378 DOI: 10.1016/j.biomaterials.2010.07.096]

18 **Silva EC**, Terreri MT, de Castro TC, Barbosa CP, Fernandes AR, Hilário MO. Sclerotic metaphyseal lines in children and adolescents treated with alendronate. *Rev Bras Reumatol* 2010; **50**: 283-290 [PMID: 21125164]

19 **Giovanini AF**, Deliberador TM, Gonzaga CC, de Oliveira Filho MA, Göhringer I, Kuczera J, Zielak JC, de Andrade Urban C. Platelet-rich plasma diminishes calvarial bone repair associated with alterations in collagen matrix composition and elevated CD34+ cell prevalence. *Bone* 2010; **46**: 1597-1603 [PMID: 20206725 DOI: 10.1016/j.bone.2010.02.026]

Published By Baishideng Publishing Group Inc
7041 Koll Center Parkway, Suite 160, Pleasanton, CA 94566, USA
Telephone: +1-925-2238242
E-mail: bpgoffice@wjgnet.com
Help Desk: https://www.f6publishing.com/helpdesk
https://www.wjgnet.com

© 2020 Baishideng Publishing Group Inc. All rights reserved.

ISSN 2220-315x (online)

World Journal of *Experimental Medicine*

World J Exp Med 2020 March 30; 10(2): 10-25



Published by Baishideng Publishing Group Inc

World Journal of Experimental Medicine

Contents

Irregular Volume 10 Number 2 March 30, 2020

ORIGINAL ARTICLE

Basic Study

10 Neutron-activated biodegradable samarium-153 acetylacetonate-poly-L-lactic acid microspheres for intraarterial radioembolization of hepatic tumors
Wong YH, Tan HY, Kasbollah A, Abdullah BJJ, Acharya RU, Yeong CH

Contents

World Journal of Experimental Medicine

Volume 10 Number 2 March 30, 2020

ABOUT COVER

Editorial Board Member of *World Journal of Experimental Medicine*, Arnon Blum, MA, MD, Professor, Department of Medicine, Baruch-Padeh Medical Center, Azrieli Faculty of Medicine, Bar ILan University, Galilee 15208, Israel

AIMS AND SCOPE

The primary aim of the *World Journal of Experimental Medicine* (*WJEM*, *World J Exp Med*) is to provide scholars and readers from various fields of experimental medicine with a platform to publish high-quality basic and clinical research articles and communicate their research findings online.

WJEM mainly publishes articles reporting research results and findings obtained in the field of experimental medicine and covering a wide range of topics including clinical laboratory medicine (applied and basic research in hematology, body fluid examination, cytomorphology, genetic diagnosis of hematological disorders, thrombosis and hemostasis, and blood typing and transfusion), biochemical examination (applied and basic research in laboratory automation and information system, biochemical methodology, and biochemical diagnostics), *etc*.

INDEXING/ABSTRACTING

The *WJEM* is now abstracted and indexed in PubMed, PubMed Central, China National Knowledge Infrastructure (CNKI), and Superstar Journals Database.

RESPONSIBLE EDITORS FOR THIS ISSUE

Responsible Electronic Editor: *Lu-Lu Qi*

Proofing Production Department Director: *Xiang Li*

NAME OF JOURNAL
World Journal of Experimental Medicine

ISSN
ISSN 2220-315x (online)

LAUNCH DATE
December 20, 2011

FREQUENCY
Irregular

EDITORS-IN-CHIEF
Arnon Blum

EDITORIAL BOARD MEMBERS
https://www.wjgnet.com/2220-315x/editorialboard.htm

EDITORIAL OFFICE
Jia-Ping Yan, Director

PUBLICATION DATE
March 30, 2020

COPYRIGHT
© 2020 Baishideng Publishing Group Inc

INSTRUCTIONS TO AUTHORS
https://www.wjgnet.com/bpg/gerinfo/204

GUIDELINES FOR ETHICS DOCUMENTS
https://www.wjgnet.com/bpg/GerInfo/287

GUIDELINES FOR NON-NATIVE SPEAKERS OF ENGLISH
https://www.wjgnet.com/bpg/gerinfo/240

PUBLICATION MISCONDUCT
https://www.wjgnet.com/bpg/gerinfo/208

ARTICLE PROCESSING CHARGE
https://www.wjgnet.com/bpg/gerinfo/242

STEPS FOR SUBMITTING MANUSCRIPTS
https://www.wjgnet.com/bpg/GerInfo/239

ONLINE SUBMISSION
https://www.f6publishing.com

© 2020 Baishideng Publishing Group Inc. All rights reserved. 7041 Koll Center Parkway, Suite 160, Pleasanton, CA 94566, USA
E-mail: bpgoffice@wjgnet.com https://www.wjgnet.com

World Journal of Experimental Medicine

Submit a Manuscript: https://www.f6publishing.com

World J Exp Med 2020 March 30; 10(2): 10-25

DOI: 10.5493/wjem.v10.i2.10

ISSN 2220-315x (online)

ORIGINAL ARTICLE

Basic Study

Neutron-activated biodegradable samarium-153 acetylacetonate-poly-L-lactic acid microspheres for intraarterial radioembolization of hepatic tumors

Yin-How Wong, Hun-Yee Tan, Azahari Kasbollah, Basri Johan Jeet Abdullah, Rajendra Udyavara Acharya, Chai-Hong Yeong

ORCID number: Yin-How Wong (0000-0003-2421-4735); Hun-Yee Tan (0000-0002-0829-5961); Azahari Kasbollah (0000-0002-7157-7822); Basri Johan Jeet Abdullah (0000-0003-3573-5886); Rajendra Udyavara Acharya (0000-0003-2689-8552); Chai Hong Yeong (0000-0003-1572-4143).

Author contributions: Wong YH performed the majority of experiments and analyzed the data; Tan HY assisted the physicochemical and radiolabeling tests; Kasbollah A organized and supervised the neutron activation process; Abdullah BJJ, Acharya RU and Yeong CH designed and coordinated the research; Wong YH and Yeong CH wrote the paper.

Supported by Fundamental Research Grant Scheme sanctioned by the Ministry of Education, Malaysia, No. FRGS/1/2019/SKK06/TAYLOR/02/3.

Institutional review board statement: Not applicable

Institutional animal care and use committee statement: Not applicable.

Conflict-of-interest statement: The authors declared no conflict of interest.

Data sharing statement: No additional data are available.

Yin-How Wong, Basri Johan Jeet Abdullah, Rajendra Udyavara Acharya, Chai-Hong Yeong, School of Medicine, Faculty of Health and Medical Sciences, Taylor's University, Subang Jaya 47500, Selangor, Malaysia

Hun-Yee Tan, School of Biosciences, Faculty of Health and Medical Sciences, Taylor's University, Subang Jaya 47500, Selangor, Malaysia

Azahari Kasbollah, Medical Technology Division, Malaysian Nuclear Agency, Bangi 43000, Selangor, Malaysia

Rajendra Udyavara Acharya, Department of Electronics and Computer Engineering, Ngee Ann Polytechnic, Singapore 599489, Singapore

Corresponding author: Rajendra Udyavara Acharya, PhD, Professor, DEng, Department of Electronics and Computer Engineering, Ngee Ann Polytechnic, 535 Clementi Road, Singapore 599489, Singapore. aru@np.edu.sg

Abstract

BACKGROUND

Liver cancer is the 6th most common cancer in the world and the 4th most common death from cancer worldwide. Hepatic radioembolization is a minimally invasive treatment involving intraarterial administration of radioembolic microspheres.

AIM

To develop a neutron-activated, biodegradable and theranostics samarium-153 acetylacetonate (^{153}SmAcAc)-poly-L-lactic acid (PLLA) microsphere for intraarterial radioembolization of hepatic tumors.

METHODS

Microspheres with different concentrations of ^{152}SmAcAc (*i.e.*, 100%, 150%, 175% and 200% w/w) were prepared by solvent evaporation method. The microspheres were then activated using a nuclear reactor in a neutron flux of 2 × 10^{12} n/cm^2/s^1, converting ^{152}Sm to Samarium-153 (^{153}Sm) *via* ^{152}Sm (n, γ) ^{153}Sm reaction. The SmAcAc-PLLA microspheres before and after neutron activation were characterized using scanning electron microscope, energy dispersive X-ray spectroscopy, particle size analysis, Fourier transform infrared spectroscopy, thermo-gravimetric analysis and gamma spectroscopy. The *in-vitro* radiolabeling

Open-Access: This article is an open-access article that was selected by an in-house editor and fully peer-reviewed by external reviewers. It is distributed in accordance with the Creative Commons Attribution NonCommercial (CC BY-NC 4.0) license, which permits others to distribute, remix, adapt, build upon this work non-commercially, and license their derivative works on different terms, provided the original work is properly cited and the use is non-commercial. See: http://creativecommons.org/licenses/by-nc/4.0/

Manuscript source: Invited Manuscript

Received: October 20, 2019
Peer-review started: October 20, 2019
First decision: December 17, 2019
Revised: February 14, 2020
Accepted: March 1, 2020
Article in press: March 1, 2020
Published online: March 30, 2020

P-Reviewer: El-Bendary M, Mohamed SY
S-Editor: Tang JZ
L-Editor: A
E-Editor: Qi LL

efficiency was also tested in both 0.9% sodium chloride solution and human blood plasma over a duration of 550 h.

RESULTS

The SmAcAc-PLLA microspheres with different SmAcAc contents remained spherical before and after neutron activation. The mean diameter of the microspheres was about 35 μm. Specific activity achieved for [153]SmAcAc-PLLA microspheres with 100%, 150%, 175% and 200% (w/w) SmAcAc after 3 h neutron activation were 1.7 ± 0.05, 2.5 ± 0.05, 2.7 ± 0.07, and 2.8 ± 0.09 GBq/g, respectively. The activity of per microspheres were determined as 48.36 ± 1.33, 74.10 ± 1.65, 97.87 ± 2.48, and 109.83 ± 3.71 Bq for [153]SmAcAc-PLLA microspheres with 100%, 150%, 175% and 200% (w/w) SmAcAc. The energy dispersive X-ray and gamma spectrometry showed that no elemental and radioactive impurities present in the microspheres after neutron activation. Retention efficiency of [153]Sm in the SmAcAc-PLLA microspheres was excellent (approximately 99%) in both 0.9% sodium chloride solution and human blood plasma over a duration of 550 h.

CONCLUSION

The [153]SmAcAc-PLLA microsphere is potentially useful for hepatic radioembolization due to their biodegradability, favorable physicochemical characteristics and excellent radiolabeling efficiency. The synthesis of the formulation does not involve ionizing radiation and hence reducing the complication and cost of production.

Key words: Radioembolization; Samarium-153; Yittrium-90; Biodegradable microsphere; Liver tumors; Neutron activation

©The Author(s) 2020. Published by Baishideng Publishing Group Inc. All rights reserved.

Core tip: We developed and tested a neutron-activated, biodegradable samarium-153 acetylacetonate-poly-L-lactic acid microspheres formulation for radioembolization of hepatic tumors. The formulation is potentially useful for intraarterial hepatic radioembolization as an alternative to yttrium-90 microspheres due to their biodegradability, favorable physicochemical characteristics and excellent radionuclide retention efficiency. The synthesis of the formulation does not involve ionizing radiation and hence reducing the complication and cost of production.

Citation: Wong YH, Tan HY, Kasbollah A, Abdullah BJJ, Acharya RU, Yeong CH. Neutron-activated biodegradable samarium-153 acetylacetonate-poly-L-lactic acid microspheres for intraarterial radioembolization of hepatic tumors. *World J Exp Med* 2020; 10(2): 10-25
URL: https://www.wjgnet.com/2220-315x/full/v10/i2/10.htm
DOI: https://dx.doi.org/10.5493/wjem.v10.i2.10

INTRODUCTION

Liver malignancy represent the 6th most common diagnosed cancer and 4th most common death from cancer worldwide[1]. There are more than 700000 people diagnosed with primary liver malignancy annually and about 50% of the colorectal carcinoma patients may develop liver metastasis[2,3]. Surgical resection or liver transplantation has been the preferred curative treatment for solid liver malignancy, unfortunately these treatments are only effective for early stage or localized liver tumors. The symptoms of liver cancer often appeared when cancer has progressed to the intermediate or advanced stage. In fact, more than 75% of the patients are diagnosed in intermediate or advanced stages where surgical resection or liver transplantation is no longer an option[4,5]. The prognosis of unresectable liver cancer was poor in the past and the management of the disease was limited to systemic pharmacotherapy, external beam radiotherapy or palliative treatments[6].

Radioembolization is an alternative minimally invasive treatment for intermediate and advanced stage liver cancer[7,8]. The treatment takes advantage of differential blood supply for normal liver parenchyma and liver tumors. Liver tumors are usually rich in vasculature and receive blood almost exclusively from hepatic artery while the

normal liver parenchyma cells receive blood predominately (about 80%) from the portal vein[9-11]. During the treatment, microspheres within the size of 20-60 μm labelled with a radionuclide that emits short range beta radiation are intraarterially administered. The microspheres are preferentially lodged near the terminal arterioles of the tumors and induces both radiation and embolization effects. Since the beta radiations only travel a few millimeters in the tissues, the healthy liver tissues and surrounding organs receive minimal radiation, while the tumors are exposed to a tumoricidal radiation dose[12-14].

Currently, only the yttrium-90 (^{90}Y) microspheres approved by the United States Food and Drug Administration for the treatment of hepatocellular carcinoma and metastatic colorectal carcinoma. The ^{90}Y radioembolic agent are available in the forms of glass beads (TheraSphere®, BTG Interventional Medicine, United Kingdom) and resin microspheres (SIR-Spheres®, SIRTex Medical Limited, Australia)[15]. Nevertheless, there are several shortcomings that ^{90}Y microspheres need to overcome. The glass- and resin-based microspheres are biocompatible but not biodegradable, therefore the microspheres will remain in the liver permanently after administration. In addition, the density of the glass-based microsphere (3.6 g/mL) is approximately three times higher than the blood plasma (1.05 g/mL), hence it's settling velocity, injection and homogenous distribution of the glass microspheres within the tumor vascular are difficult to control[16]. ^{90}Y is a pure beta emitter and does not carry any imaging properties, evaluation of extrahepatic activity and liver dosimetry post-administration is often performed on ^{90}Y Bremsstrahlung single-photon emission computed tomography or positron emission tomography imaging that shows low quantitative accuracy or sensitivity[17]. Furthermore, ^{90}Y is commonly produced using a high-cost strontium-90 generator associated with complicated chemical separation process[18].

Samarium-153 (^{153}Sm) is a potential radionuclide that can be used for hepatic radioembolization. ^{153}Sm can be produced from its non-radioactive isotope, ^{152}Sm *via* neutron activation, *i.e.*, ^{152}Sm (n, γ) ^{153}Sm. The ^{153}Sm has been used for palliative pain treatment for bone metastases and radiosynovectomy in the past decades. The imaging properties of ^{153}Sm have been demonstrated in some previous studies of pharmacoscintigraphy and gastrointestinal imaging research[19-21]. The simultaneous emission of beta and gamma radiations from ^{153}Sm has rendered it a potential theranostic radionuclide for targeted cancer therapy.

This study aimed to develop a biodegradable radioembolic microspheres formulation loaded with ^{153}Sm to overcome the limitations of ^{90}Y microspheres for hepatic radioembolization. The physicochemical characteristics, radioactivity, radioimpurities as well as ^{153}Sm retention efficiency of the developed microspheres were studied and discussed in the following sections.

MATERIALS AND METHODS

Poly-L-lactic acid (PLLA) (viscosity = 0.8-1.2 dL/g), Samarium-152 acetylacetonate (^{152}SmAcAc) (99% purity) and polyvinyl alcohol (PVA, average molecular weight = 67000) were procured from Sigma Aldrich (St. Louis, MI, United States). Analytical grade chemicals and deionized water were used in all the experiments unless stated otherwise.

Preparation of ^{152}SmAcAc-PLLA microspheres

^{152}SmAcAc-PLLA microspheres with different concentrations of ^{152}SmAcAc were prepared using oil-in-water solvent evaporation method[22]. Firstly, 20 mL of chloroform solution containing 1.0 g of PLLA and different amounts of ^{152}SmAcAc (*i.e.*, 1.0 g, 1.5 g, 1.75 g and 2.0 g) were added dropwise into 600 mL of 3% (w/v) PVA solution under overhead stirring at 950 rpm. The overhead stirring was continued for 12 h to allow evaporation of the chloroform. The resulting ^{152}SmAcAc-PLLA microspheres were then collected through vacuum filtration using a filter paper of 15 μm pores. Zero point one mol/L hydrochloride acid (HCl) and distilled water were used to dissolve and wash off any unbound ^{152}SmAcAc from the formulation. Subsequently, the microspheres were dried in a vacuum oven at room temperature for 48 h. Once the microspheres were completely dried, they were fractionated into 20-60 μm diameter using stainless steel sieves. Finally, the microspheres within 20-60 μm diameter were collected and stored in a sealed vial at –20 °C for further analysis.

Neutron activation of ^{152}SmAcAc-PLLA microspheres

The ^{152}SmAcAc-PLLA microspheres were sent for neutron activation using a 750 kW pool-type research reactor (TRIGA Mark II, General Atomics, CA, United States). Prior to neutron activation, the samples were transferred into a polyethylene vial and

sealed. The samples were neutron-activated using either the pneumatic transfer system (PTS) or rotary specimen rack (RR) method. The neutron activation protocols for both PTS and RR methods are given in Table 1. The radioactivity of the neutron-activated samples was measured using a calibrated dose calibrator (CRC 25R, Capintec, NJ, United States). The activity per microsphere was calculated by dividing the sample activity with the estimated number of microspheres present in the sample.

Physicochemical characterization of SmAcAc-PLLA microspheres before and after neutron activation

Physicochemical characterization of the SmAcAc-PLLA microspheres before and after neutron activation was carried out using scanning electron microscopy (SEM), energy dispersive X-ray (EDX) spectroscopy, particle size analyzer, Fourier transform infrared spectroscopy (FTIR), thermo-gravimetric analysis (TGA) and wavelength dispersive X-ray fluorescence (WDXRF) spectrometry. The objectives and methods of each test were elaborated in the following sections.

SEM and EDX spectroscopy: Surface morphology of the SmAcAc-PLLA microspheres before and after neutron activation was examined using a SEM system (Quanta FEG 450, FEI, Oregon, United States). SEM images were obtained at 5 kV, 10 mm working distance and 2.0 spot size. Elemental compositions of the SmAcAc-PLLA microspheres before and after neutron activation were analyzed using EDX spectroscopy on the SEM system. The samples were mounted on aluminum stubs before performing the SEM and EDX analysis.

Laser scattering particle size analysis: The mean diameter and particle size distribution of the PLLA and SmAcAc-PLLA microspheres before and after neutron activation were determined using a laser scattering particle size distribution analyzer (Microtrac X100, Microtrac, United States). Microspheres samples suspended in distilled water were ultrasonicated before loading into the particle size analyzer for measurement.

FTIR spectroscopy: FTIR spectroscopy was performed to identify the chemical bonds of the microspheres. FTIR spectra within 600-4000 cm^{-1} of the PLLA, ^{152}SmAcAc and ^{152}SmAcAc-PLLA microspheres were obtained on a calibrated FTIR spectrometer (Spectrum 100, PerkinElmer Inc., MA, United States). Firstly, the samples were mixed with spectroscopy grade potassium bromide grain and dried in an oven to remove absorbed moisture. The potassium bromide-mixed samples were then pressed into pellets using designated tools provided by the manufacturer (PerkinElmer Inc., MA, United States) and subjected for FTIR analysis.

TGA: Thermal profiles of the ^{152}SmAcAc-PLLA microspheres were studied using a TGA 8000™ analyzer (PerkinElmer Inc., MA, United States). The profiles of its raw materials, PLLA and ^{152}SmAcAc, were also included for comparison. Approximately 5 mg of the sample was transferred into a ceramic sample pan and placed inside the TGA analyzer. The sample was then heated under nitrogen flow from 30–800 °C at a rate of 10 °C/min. TGA profiles of the samples were analyzed using the dedicated software (Pyris, PerkinElmer Inc., MA, United States).

WDXRF spectrometry: The amount of ^{152}Sm presence in the ^{152}SmAcAc-PLLA microspheres with different ^{152}SmAcAc weight (1.0 g, 1.5 g, 1.75 g and 2.0 g) were determined using the semi-quantitative analysis of WDXRF spectrometry (Zetium, Malvern PANanalytical Ltd., Royston, United Kingdom).

Gamma spectroscopy

Gamma spectroscopy was performed at 24 h after neutron activation using a coaxial, p-type hyperpure germanium detector (Canberra, Meriden, United States) to identify the radionuclides present in the formulation. The sample was placed at a calibrated distance in the hyperpure germanium detector and counted for 5 min live time. The gamma spectrum was obtained and analyzed using dedicated software (Genie™ 2000 Ver. 3.2, Canberra, United States).

Density and viscosity measurements

The density of the ^{152}SmAcAc-PLLA microspheres were determined based on Archimedes principle. The density was calculated based on the relation given in Equation (1). Mettler Toledo (ME 204) density meter (Ohio, United States) was used for this purpose.

(1) Density of Microspheres (ρ_s) = $M_b \times \rho_w$ / (M_a - M_w)

Where M_b is the mass of the sample on a balance, M_a is the mass of the sample in air, M_w is the mass of the sample in water and is the density of water (1 g/cm^3).

Table 1 Neutron activation protocols for activation of samarium acetylacetonate-poly-L-lactic acid microspheres

Protocol	Pneumatic transfer system	Rotary specimen rack
Thermal neutron flux, θ_{th} (n/cm^2/s)	5.0 x 10^{12}	2.0 x 10^{12}
Maximum duration of neutron activation	Up to 5 min	Up to 6 h
Location of neutron activation	Near to the core	Peripheral to the core
Sample delivery	Automatic	Manual

The ρ_s was used to estimate the number of microspheres per gram of sample using Equation (2).

(2) Number of particles per gram = $6 \times 10^{12} / (\pi \times \rho_s \times Dp^3)$

Where D*p* is the mean diameter of the microspheres in μm and ρ_s is the density of the microspheres in g/cm^3.

The viscosity, η_o of [153]SmAcAc-PLLA microspheres [2.5% (w/v)] suspended in sodium chloride (NaCl) solution was measured at 37 °C using a rheometer (HAAKE MARS, Thermo Fisher Scientific, MA, United States). The reading was then incorporated into the Stokes' Law to calculate the sedimentation rate (settling velocity)[13].

(3) $V_{sed} = g \times Dp^2 \times (\rho_s - \rho_f) / (18 \times \eta o)$

Where V_{sed} is the sedimentation rate (cm/s), *g* is the gravitational acceleration constant (981 cm/s^2) and η_o is the dynamic viscosity of the fluid (ρ_f = g/cm/s).

In-vitro radiolabeling efficiency test

The radiolabeling efficiency of the neutron-activated [153]SmAcAc-PLLA microspheres was tested in both 0.9% NaCl solution and human blood plasma over a period of 550 h. The microspheres were suspended in the test solutions and continuously mixed at 50 rpm for 1 h using a roller mixer. The samples were then centrifuged at 2000 rpm for 10 min. One milliliter of the supernatant was then collected and assayed using an automated gamma counter (2470 Wizard^2, PerkinElmer, MA, United States). The procedures were repeated until 8 mL of assay samples were collected over a period of 550 h[22].

RESULTS

Synthesis of [152]SmAcAc-PLLA microspheres

The [152]SmAcAc-PLLA microspheres loaded with different amount of [152]SmAcAc (1.0 g, 1.5 g, 1.75 g and 2.0 g) were successfully synthesized using the solvent evaporation method. The synthesis parameters such as stirring rate (950 rpm), PVA concentration (3% w/v) and polymer solution concentration were optimized in this study in order to produce microspheres with a mean diameter of approximately 35 μm and size distribution within 20-60 μm.

Neutron activation

The [152]SmAcAc-PLLA microspheres were neutron-activated using two different methods: (1) Automatic PTS control where the samples were sent near to the reactor core and neutron-activated for a maximum duration of 5 min; and (2) Manual loading RR method where the samples were neutron-activated for an extended duration of 3 h and 6 h at the peripheral location from the reactor core. Table 1 shows the neutron activation protocols for both PTS and RR methods. The specific activity (GBq/g) achieved for different formulations and neutron activation methods are given in Figure 1. The radioactivity increased linearly with the amount of [152]SmAcAc in the formulations. However, the maximum amount of [152]SmAcAc that can be loaded to the PLLA microsphere was 200% (w/w), and this achieved the maximum specific activity of 6.40 ± 0.07 GBq/g for a 6 h neutron activation using RR method. The radioactivity was proportional to the neutron activation time as theoretically known.

Physicochemical characterization of SmAcAc-PLLA microspheres before and after neutron activation

Figure 2 shows the SEM images of the PLLA and SmAcAc-PLLA microspheres before and after neutron activation. Spherical microspheres were successfully produced following oil-in-water solvent evaporation synthesis. There is no [152]SmAcAc crystals were seen on the surface of the microspheres even at the highest concentration of

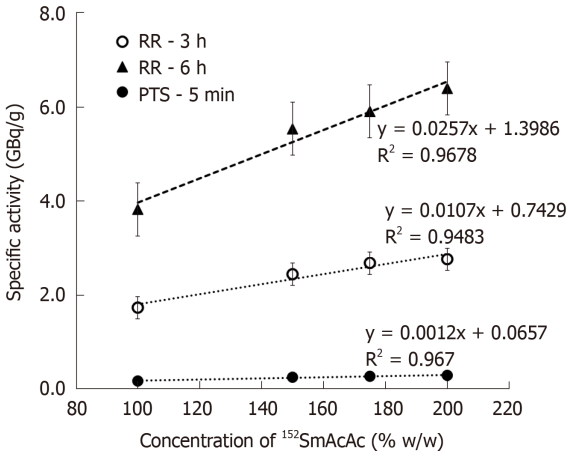


Figure 1 Specify activity of samarium acetylacetonate-poly-L-lactic acid microspheres (100%, 150%, 175% and 200%, w/w samarium acetylacetonate), neutron-activated using different neutron activation protocol and duration. SmAcAc: Samarium acetylacetonate; RR: Rotary specimen rack; PTS: Pneumatic transfer system.

^{152}SmAcAc. In addition, the washing process using diluted HCl did not cause any physical damage to the microspheres. A prolonged neutron activation time of 6 h in the thermal neutron flux of 2.0 × 10^{12} n/cm^2/s^1 has produced physical damage and fragmentation on the microspheres. The damage and fragmentation were more severe at higher concentration of ^{152}SmAcAc. Nonetheless, neutron activation time of 3 h in the same neutron flux setting did not damage the physical structure of the microspheres. An extended part of the study has been carried out and found that neutron activation time longer than 4 h would cause physical damage and fragmentation of the PLLA microspheres (data were not included in this manuscript).

Figure 3 shows the EDX spectrum of the PLLA microspheres and SmAcAc-PLLA microspheres before and after 3 h neutron activation. The spectra show the presence of carbon (C) and oxygen (O) in the PLLA microspheres, and C, O and Sm in the SmAcAc-PLLA microspheres. No other element was detected after neutron activation for both microspheres. The hydrogen (H) presence in the microspheres could not be detected by EDX due to the limitation of EDX in detecting any chemical element lower than atomic number of 6. In addition, no constituent of chloride from the diluted HCl washing was detected on the EDX spectrum of the SmAcAc-PLLA microspheres.

The mean diameter and size distribution of the PLLA and SmAcAc-PLLA microspheres before and after 3 h neutron activation are presented in Figure 4. The mean diameter of the PLLA microspheres was 34.45 ± 0.20 μm and the size distribution was within 20 μm and 60 μm. Different concentrations of ^{152}SmAcAc in the PLLA microspheres did not change the size distribution significantly, however the mean diameter increased slightly with the amount of ^{152}SmAcAc loaded to the polymer. For instance, the mean diameter increased from 34.85 ± 0.17 μm to 38.25 ± 0.15 μm when the amount of ^{152}SmAcAc increased from 100% to 200% w/w. The mean diameter of the microspheres was not altered significantly after 3 h neutron activation.

Figure 5 shows the FTIR spectrum of the PLLA (Figure 5A), ^{152}SmAcAc-PLLA microspheres (Figure 5B-E) and ^{152}SmAcAc crystal (Figure 5F). The FTIR spectrum of the ^{152}SmAcAc crystal shows IR bands in the C=C and C=O regions (1700-1500 cm^{-1}) (Figure 5F)[23-25]. The FTIR spectra of the ^{153}SmAcAc-PLLA microspheres indicated that the C=C vibration of acetylacetonate was noticed at 1515 cm^{-1}, similar to the wavelength for ^{152}SmAcAc crystals. On the other hand, the C=O region of the acetylacetonate was shifted from 1580 cm^{-1} in the ^{152}SmAcAc to 1610 cm^{-1} in the SmAcAc-PLLA microspheres (Figure 5B-E). This indicates that the PLLA carbonyl groups are interacting with the ^{152}SmAcAc complex, resulting in the immobilization of the ^{152}SmAcAc complex in the PLLA matrix. This in turn explains the low release characteristics of the ^{153}SmAcAc-PLLA microspheres. There was no band signal observed at these wavelengths in the FTIR spectrum of the PLLA microspheres (Figure 5A). In addition, there was no noticeable change in the C=O band of the PLLA (1760 cm^{-1}) since any shift would be masked by the strong absorption band of the remaining, non-coordinating C=O bonds.

Figure 6 shows the TGA profile of the PLLA, ^{152}SmAcAc-PLLA microspheres and ^{152}SmAcAc crystal. The PLLA microspheres showed only one event of mass loss, which can be ascribed to the decomposition of polymer main chain starting from 250 °C. The TGA profile of the ^{152}SmAcAc crystal shows multiple steps decomposition

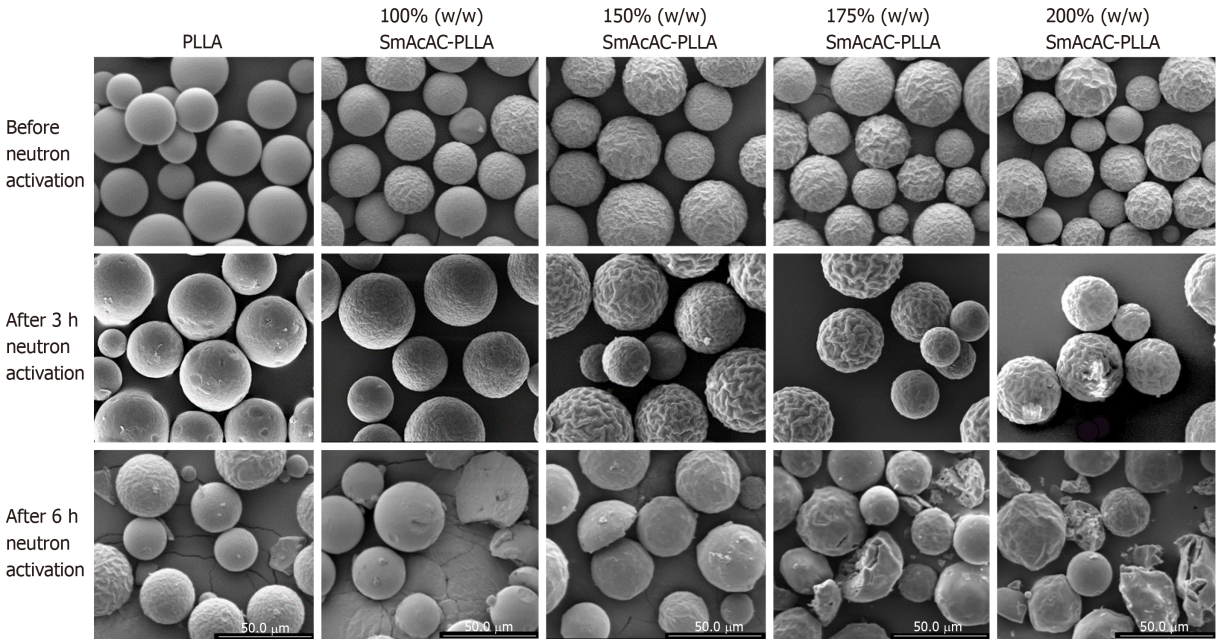


Figure 2 Scanning electron microscopy images of the poly-L-lactic acid and samarium acetylacetonate-poly-L-lactic acid microspheres before and after 3 h and 6 h neutron activation. Scale bars are 50.0 μm. PLLA: Poly-L-lactic acid; SmAcAc: Samarium acetylacetonate.

with the remaining residual weight indicating the presence of about 40% ^{152}Sm in the crystal. On the other hand, the TGA profiles of the ^{152}SmAcAc-PLLA microspheres show additional decomposition steps at above 200 °C, indicating decomposition of ^{152}SmAcAc above this temperature. Loading of ^{152}SmAcAc crystal to the PLLA polymer matrix has reduced the decomposition temperature from 250 °C to 200 °C. The residual weight presence in the ^{152}SmAcAc-PLLA microspheres indicated the presence of ^{152}Sm in the sample. The ^{152}Sm content in the ^{152}SmAcAc-PLLA microspheres was corresponded to the ^{152}Sm content (between 12% and 18%) as determined by WDXRF (Table 2).

Gamma spectroscopy

Figure 7 shows the gamma spectrum of the ^{153}SmAcAc-PLLA microspheres acquired at 24 h after neutron activation. Several photopeaks were observed at 41 keV, 47 keV, 69 keV and 103 keV on the gamma spectrum of the ^{153}SmAcAc-PLLA microspheres. The most dominant photopeak was found at 103 keV followed by a smaller photopeak at 69 keV. These energies corresponded to the principal gamma energies emitted by ^{153}Sm. The other two photopeaks (41 keV and 47 keV) were the K-shell characteristic X-rays emitted following internal conversion of ^{153}Sm. The gamma spectroscopy results were in accordance with the EDX spectroscopy results, showing no radionuclide impurities on the ^{152}SmAcAc-PLLA microspheres after neutron activation

Density and viscosity measurement

The density of the ^{152}SmAcAc-PLLA microspheres ranged from 1.25 g/cm^3 to 1.35 g/cm^3 depending on the amount of the ^{152}SmAcAc added in the formulation (Table 2). The density values thus obtained were used to determine the number of microspheres per gram using Equation (2) given in the Methods section and the results are presented in Table 2. The number of microspheres per gram is inversely proportional to the density and diameter of the microspheres. Since the density and diameter of the ^{153}SmAcAc-PLLA microspheres increased when the amount of ^{152}SmAcAc increased, this results in a reduction of the number of microspheres per gram for the formulation with increased ^{152}SmAcAc concentration. For example, 37 million microspheres were estimated in a gram of ^{153}SmAcAc-PLLA microspheres loaded with 100% (w/w) ^{152}SmAcAc, while only 24 million microspheres were estimated in the 200% (w/w) SmAcAc. The activity per microsphere was estimated as 46.31 ± 1.39, 81.01 ± 1.52, 95.40 ± 2.59, and 114.37 ± 3.60 Bq for the formulations loaded with 100%, 150%, 175% and 200% (w/w) ^{152}SmAcAc, respectively.

The viscosity of the microspheres suspension at 2.5% (w/v) concentration at 37 °C are shown in Figure 8. As demonstrated in the graph, the viscosity of the ^{152}SmAcAc-PLLA suspension at different shear rates were substantially similar and hence the

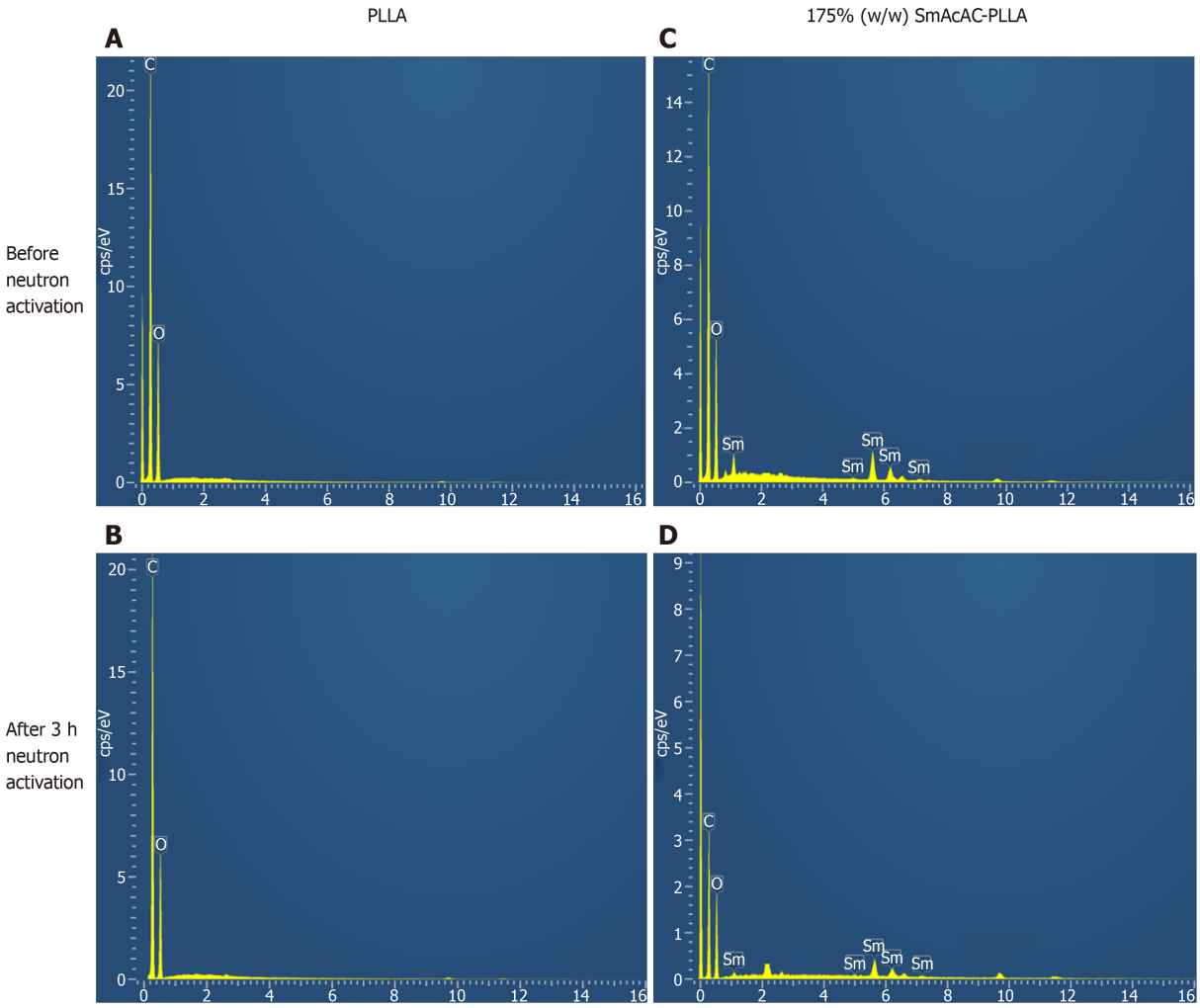


Figure 3 The energy dispersive X-ray spectrum of the poly-L-lactic acid microspheres and samarium acetylacetonate-poly-L-lactic acid microspheres before and after 3 h neutron activation. A and B: Energy dispersive X-ray spectrum of the poly-L-lactic acid (PLLA) microspheres; C and D: samarium acetylacetonate (SmAcAc)-PLLA microspheres. Energy dispersive X-ray spectrum of the PLLA and SmAcAc-PLLA microspheres before and after 3 h neutron activation clearly show the presence of carbon and oxygen in the PLLA microspheres; and carbon, oxygen and Sm in the SmAcAc-PLLA microspheres. PLLA: Poly-L-lactic acid; SmAcAc: Samarium acetylacetonate.

average viscosity value was used to represent the viscosity of the respected microspheres suspension (Figure 8). The settling velocity (cm/s) of the formulation is depending on the viscosity, density and size of the microspheres. The settling velocity of ^{153}SmAcAc-PLLA are given in Table 2.

In-vitro radiolabeling efficiency

The *in-vitro* radiolabeling of ^{153}SmAcAc-PLLA microspheres tested in 0.9% NaCl solution and human blood plasma is demonstrated in Figure 9. The formulation showed excellent ^{153}Sm retention of more than 99% in 0.9% NaCl solution and human blood plasma over a test period of 550 h. A slightly lower ^{153}Sm retention efficiency was observed in human blood plasma than in the 0.9% NaCl solution but the difference was negligible (less than 1%).

DISCUSSION

Radioembolization with the use of radiolabelled microspheres has several advantages over external beam radiotherapy for hepatic malignancies. Firstly, it treats liver tumors by dual-mechanism pathways: Embolization (blocking blood supply to the liver tumors) and internal radiation therapy using high energy short-range radiations such as beta[26]. Secondly, it is useful to treat diffuse hepatocellular carcinoma or liver metastasis when surgery or local treatment is not possible. Thirdly, it minimizes radiation damage to the surrounding healthy tissues[27]. Current formulations approved by the United States Food and Drug Administration for radioembolization

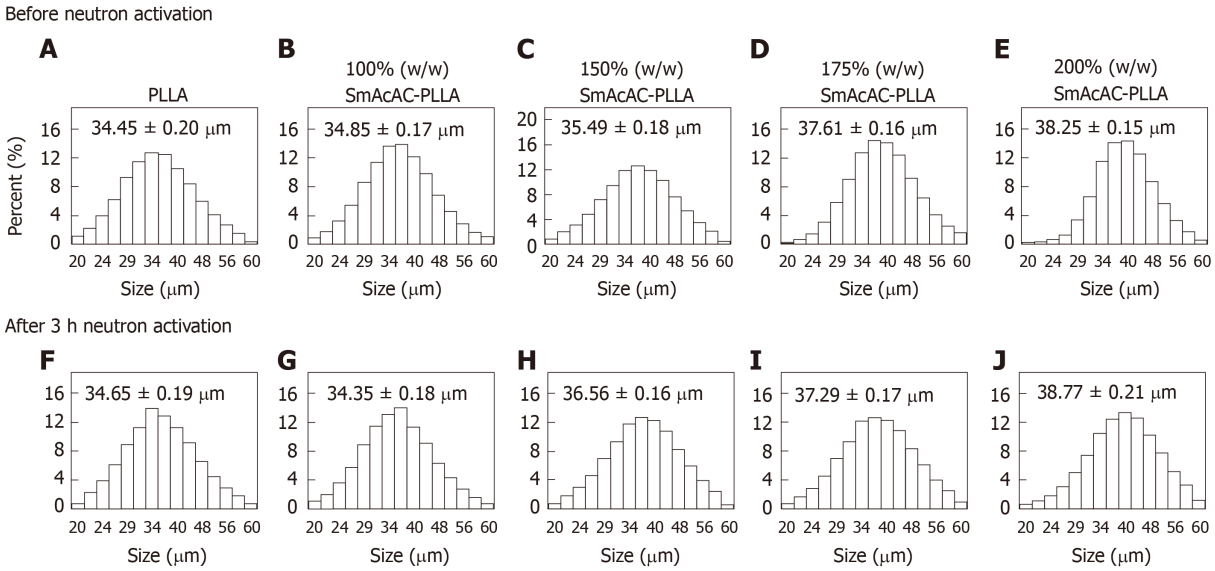


Figure 4 Particle size distribution of the poly-L-lactic acid and samarium acetylacetonate- poly-L-lactic acid microspheres before and after 3 h neutron activation. A-E: Before neutron activation; F-J: After 3 h neutron activation. PLLA: Poly-L-lactic acid; SmAcAc: Samarium acetylacetonate.

of liver metastasis are resin-based (SIR-Sphere) and glass-based (TheraSphere) microspheres labelled with pure beta emitter, ^{90}Y. Several researches have been conducted to explore alternative radionuclides and polymers to overcome some limitations of the ^{90}Y microspheres[28-32]. A theranostic radionuclide that emits both beta and gamma radiations is preferred to facilitate treatment planning and dosimetry. Compared to the generator-based radionuclide production, neutron activation is a preferred method due to its relatively lower cost of production, simpler process, wider availability of nuclear reactors globally and reduces international shipping of radioactive products. Examples of neutron-activated radionuclides include ^{166}Ho, ^{177}Lu, ^{186}Re and ^{188}Re. Biodegradable polymer is also favored in order to minimize the risk of long-term complications such as hepatitis and cirrhosis.

This study aimed to develop a biodegradable PLLA microspheres loaded with stable ^{152}SmAcAc. The microspheres were then activated using a nuclear reactor to produce radioactive ^{153}SmAcAc-PLLA microspheres that emits both beta ($E_{\beta\text{-max}}$ = 810 keV) and gamma (103 keV) radiations, potentially useful for theranostic radioembolization of liver malignancies. PLLA is biocompatible for human body and its degradation reaction is mainly due to hydrolysis to lactic acid. The lactic acid produced during the biodegradation of PLLA can serve as an energy substrate for cells and has been shown to have antioxidant properties[33]. In addition, the PLLA has a near blood plasma density and thus could overcome the high density drawback from glass-based ^{90}Y microspheres[28]. The developed ^{153}SmAcAc-loaded PLLA microspheres formulation combines the benefits of being biocompatible, biodegradable, similar density to human blood plasma, and emitting both therapeutic and diagnostic radiations (theranostic). Moreover, the production cost is reduced due to the relatively easier and cheaper neutron activation method.

A simple one-step oil-in-water solvent evaporation technique was used in this study to incorporate ^{152}SmAcAc crystals into the PLLA polymer. The ^{152}Sm was complexed with the acetylacetonate ligand to enable its incorporation into PLLA *via* oil-in-water solvent evaporation[34]. The ^{152}SmAcAc, ranging from 100 to 200% (w/w), was successfully encapsulated into the PLLA microspheres. Incorporation of ^{152}SmAcAc beyond 200% (w/w) has resulted in irregular shape of the microspheres with excessive unbound ^{152}SmAcAc crystals on the surface. The morphology and diameter of the microspheres were known to be affected by several synthesis parameters such as concentration of PVA and stirring rates, in which, a lower PVA concentration and stirring rate would produce microspheres with larger mean diameter and size distribution[35]. The optimum PVA concentration of 3% (w/w) and stirring rate of 950 rpm have resulted in spherical microspheres with a mean diameter of approximately 35 μm. The microspheres were sieved to obtain the size within 20-60 μm diameter, which is a strict requirement for intraarterial hepatic radioembolization[10].

The integrity of the ^{153}SmAcAc-loaded PLLA microspheres after neutron activation is important to ensure its safe administration into human body. Several factors such as moisture content and neutron activation time are known to produce detrimental

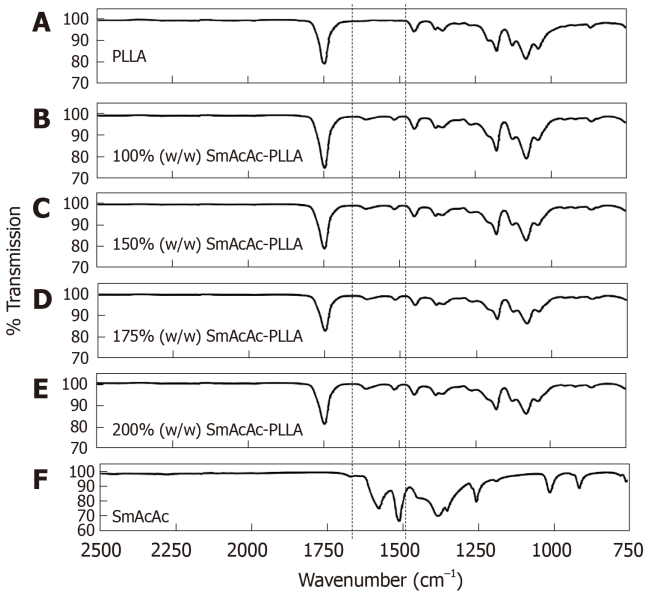


Figure 5 Fourier transform infrared spectroscopy spectrum of the poly-L-lactic acid, samarium acetylacetonate-poly-L-lactic acid microspheres, and samarium-152 acetylacetonate crystal. A: Fourier transform infrared spectroscopy (FTIR) spectrum of the poly-L-lactic acid; B-E: FTIR spectrum of the samarium acetylacetonate-poly-L-lactic acid microspheres; F: FTIR spectrum of the samarium-152 acetylacetonate crystal. PLLA: Poly-L-lactic acid; SmAcAc: Samarium acetylacetonate.

effects on the integrity of the PLLA microspheres[32]. In order to prevent deterioration during neutron activation, the formulations were dried in a vacuum oven for at least 48 h to remove any excessive moisture prior to neutron activation. The ^{153}SmAcAc-PLLA microspheres remained intact and spherical with similar size distribution after 3 h neutron activation but was fragmented when the neutron activation time was prolonged to 6 h. The formulation with a higher loading of ^{152}SmAcAc would experience a greater extent of fragmentation. The fragmentation maybe ascribed to the radiation damage to the PLLA microspheres. Similar fragmentation of PLLA microspheres after neutron activation has been observed in a previous study[32]. From the results of this study, the optimum neutron activation time for neutron activation of ^{152}SmAcAc-PLLA microspheres under a thermal neutron flux of 2×10^{12} n/cm^2/s^1 was determined as 3 h.

In order to facilitate intraarterial injection *via* a microcatheter, the radioembolic microspheres are usually suspended in 0.9% NaCl solution or distilled water. The ^{153}SmAcAc-PLLA microspheres suspension has a similar viscosity to the 0.9% NaCl solution (0.01 g/cm/s) but slightly lower than the viscosity of the human blood (0.03 g/cm/s)[36]. Owing to its lower density, the settling velocity of the ^{153}SmAcAc-PLLA microspheres suspension was relatively lower compared to the glass- and resin-based microspheres[28,29,37]. A lower settling velocity could prevent the microspheres from settling in the microcatheter or blood vessels during administration and enable a more homogenous distribution of the microspheres within the tumor volume. The retention efficiency of radioactive ^{153}Sm in the microspheres was excellent (> 99%) tested in both 0.9% NaCl solution and human blood plasma for an extended period of 550 h. High retention efficiency is required to minimize leakage of free ^{153}Sm to other parts of the body. The excellent retention efficiency of the formulation can be ascribed to the interaction between the carbonyl groups of PLLA with the ^{153}SmAcAc complex, which has resulted in the immobilization of the ^{153}SmAcAc complex in the PLLA matrix.

^{152}SmAcAc-PLLA microspheres with different concentrations of ^{152}SmAcAc, ranging from 100%–200% w/w, were tested in this study. Higher concentration of ^{152}SmAcAc is preferred to increase the specific activity of each microsphere. However, higher loading of ^{152}SmAcAc would increase the density and mean diameter of the microsphere. In addition, it also increased the difficulties in removing the unbound ^{152}SmAcAc. Therefore, it is important to find the optimum concentration of ^{152}SmAcAc to be loaded to each PLLA microsphere to achieve the desired properties for radioembolization of liver tumors. According to the results of this study, 175% (w/w) ^{152}SmAcAc is recommended as it produces microspheres with mean diameter of 37 μm and specific activity of 95 Bq per microsphere. This value is in between the protocols used in SIR-Sphere (40-70 Bq per microsphere) and TheraSphere (2500 Bq per microsphere). A further increase in the ^{152}SmAcAc concentration (*e.g.*, from 175% to

Table 2 Physicochemical properties of the neutron-activated samarium-153 acetylacetonate-poly-L-lactic acid microspheres

Physicochemical properties	100% (w/w) [153]SmAcAc-PLLA	150% (w/w) [153]SmAcAc-PLLA	175% (w/w) [153]SmAcAc-PLLA	200% (w/w) [153]SmAcAc-PLLA
Mean diameter (μm)	34.35 ± 0.18	36.56 ± 0.16	37.29 ± 0.17	38.77 ± 0.21
Density (g/cm^3)	1.25 ± 0.030	1.29 ± 0.006	1.31 ± 0.047	1.35 ± 0.068
Number of microspheres per g	37 million	30 million	28 million	24 million
Settling velocity (cm/s)	0.016 ± 0.0004	0.019 ± 0.0002	0.022 ± 0.0003	0.027 ± 0.0004
Specific activity (GBq/g)	1.74 ± 0.05	2.45 ± 0.05	2.69 ± 0.07	2.77 ± 0.09
Activity per particle (Bq)	46.31 ± 1.33	81.01 ± 1.65	95.40 ± 2.48	114.37 ± 3.72
Samarium content (%)	12.06 ± 0.69	14.56 ± 0.28	16.32 ± 0.34	17.28 ± 0.46

[153]SmAcAc-PLLA: Samarium-153 acetylacetonate-poly-L-lactic acid.

200%) produced a relatively small increment (about 3%) in the radioactivity but has further increased the mean diameter and density of the microspheres, resulting in reduced number of microspheres and increased settling velocity. In addition, higher amount of [152]SmAcAc would also increase the difficulties in removing the unbound [152]SmAcAc. Although a more concentrated HCl solution could be used during washing, this might cause structural damage to the PLLA. Therefore, the 175% (w/w) [152]SmAcAc is recommended over the 200% (w/w) [152]SmAcAc.

Although the specific activity (GBq/g) of the [153]SmAcAc-PLLA microspheres was slightly lower than the target therapeutic dose of 3.0 GBq per vial in [90]Y microspheres, administration of larger number of microspheres with medium specific activity has been suggested earlier[31] to produce better therapeutic efficacy than lower number of microspheres with higher specific activity. This is because a more even distribution of the radiation dose within the tumor volume is expected by a larger number of microspheres with lower specific activity while achieving the same total therapeutic dose prescribed for the treatment (total activity = number of microspheres x specific activity per microsphere). Nevertheless, a detailed dosimetry and treatment planning software are needed to determine the optimum dosage/approach for each individual patient. If necessary, the enriched form of [152]Sm (about 99% [152]Sm) can be used to replace the natural abundance [152]Sm (about 27% [152]Sm) if higher specific activity is desired. The radioactivity produced by the enriched [153]Sm is expected to be around three to four times higher than the natural abundant [153]Sm.

Production of radioactive formulations using neutron activation technique could possibly reduce the production cost and make the treatment more affordable across many nations. The commercially available [90]Y is produced from strontium-90, a fission product of uranium in a nuclear reactor, by chemical high-purity separation. The elution and radiolabeling process involves multiple steps involving advanced technology and skills. It also increases radiological burden to the personnel as the whole production process is done under radioactive environment[18]. In comparison, the preparation of [152]SmAcAc-PLLA microspheres is relatively easier, cheaper and does not involve ionizing radiation as non-radioactive form of [152]Sm is used during the synthesis process. The formulation can be kept and only sent for neutron activation when needed. According to the latest International Atomic Energy Agency Research Reactor Database, there are 224 research reactors currently operates across 53 countries[38]. If the formulation can be activated locally, it would significantly reduce cross-borders radioactive shipments and lead time hence more radioembolization patients can be benefited. Some studies have suggested using neutron-activated [188]Re and [166]Ho as a substitute to [90]Y, however these radionuclides have relatively short half-life, *i.e.*, 17 h and 26 h, respectively. In our opinion, [153]Sm has an ideal half-life of 46.3 h and it emits both therapeutic beta energies and diagnostic range gamma radiation, renders it a useful theranostics agent for liver radioembolization. Furthermore, it is readily available in a stable chemical form ([152]Sm, natural abundance 26%) and decays into a stable daughter ([153]Eu), hence minimizing the risk of radioactive waste.

In conclusion, a biocompatible, biodegradable [152]SmAcAc-PLLA microspheres was successfully developed in this study. The microspheres have a mean diameter of approximately 37 μm and size distribution between 20 μm and 60 μm. The microspheres achieved a specific activity of 98 Bq per microsphere for the formulation loaded with 175% (w/w) [152]SmAcAc. No significant radionuclide impurities were found and the [153]Sm retention efficiency was above 99% when tested in 0.9% NaCl

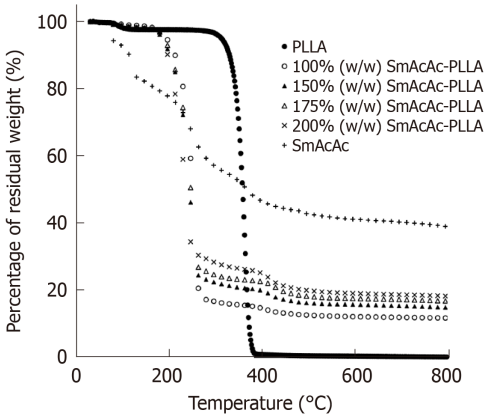


Figure 6 Thermo-gravimetric analysis profiles of poly-L-lactic acid, samarium-152 acetylacetonate, and samarium-152 acetylacetonate-poly-L-lactic acid microspheres. PLLA: Poly-L-lactic acid; SmAcAc: Samarium acetylacetonate.

solution and human blood plasma for 550 h. Further studies are needed to complete the dosimetry and to compare the radioembolization efficiency with the commercially available formulations.

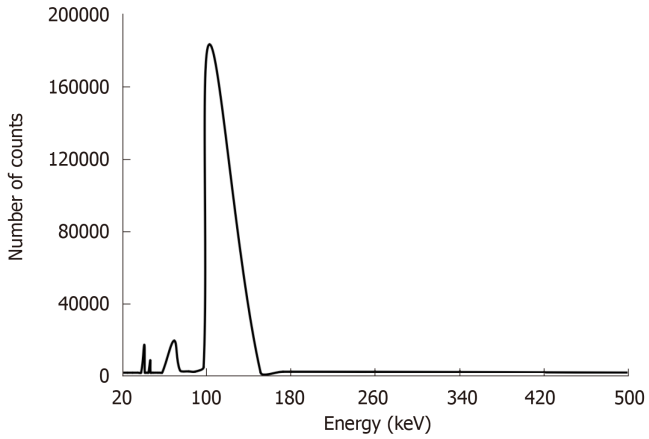


Figure 7 Gamma spectrum of samarium-153 acetylacetonate-poly-L-lactic acid microspheres at 24 h post neutron activation.

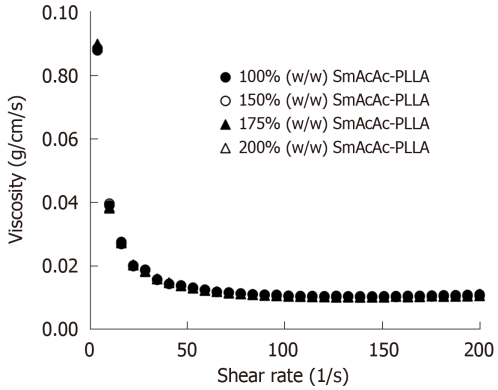


Figure 8 The viscosity of samarium acetylacetonate-poly-L-lactic acid microspheres suspension at various shear rate. The microspheres suspension (2.5% w/v) were prepared in 0.9% sodium chloride solution at 37 °C. PLLA: Poly-L-lactic acid; SmAcAc: Samarium acetylacetonate.

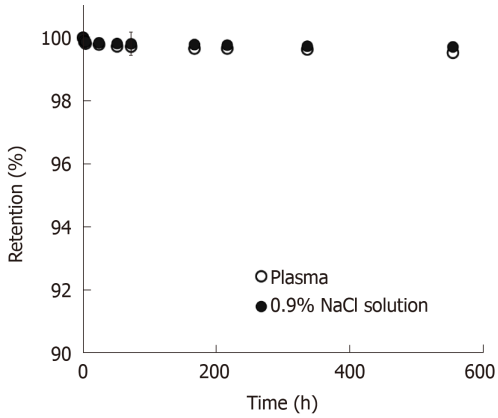


Figure 9 Retention (%) of samarium-153 in neutron-activated samarium-153 acetylacetonate-poly-L-lactic acid microspheres suspended in 0.9% sodium chloride solution and human blood plasma over a duration of 550 h. NaCl: Sodium chloride.

ARTICLE HIGHLIGHTS

Research background

Liver cancer is the 6th most common cancer in the world and the 4th most common death from cancer worldwide. Hepatic radioembolization is a minimally invasive treatment involving intraarterial administration of radioembolic microspheres.

Research motivation

To develop a novel radioembolic microspheres formulation as an alternative to Yttrium-90 microspheres for intraarterial hepatic radioembolization.

Research objectives
To develop a neutron-activated, biodegradable and theranostics samarium-153 acetylacetonate (^{153}SmAcAc)-poly-L-lactic acid (PLLA) microsphere for intraarterial radioembolization of hepatic tumors.

Research methods
Microspheres with different concentrations of ^{152}SmAcAc (*i.e.*, 100%, 150%, 175% and 200% w/w) were prepared by solvent evaporation method. The microspheres were then activated using a nuclear reactor in a neutron flux of 2×10^{12} n/cm^2/s^1, converting ^{152}Sm to Samarium-153 (^{153}Sm) *via* ^{152}Sm(n, γ) ^{153}Sm reaction. The SmAcAc-PLLA microspheres before and after neutron activation were characterized using scanning electron microscope, energy dispersive X-ray spectroscopy, particle size analysis, Fourier transform infrared spectroscopy, thermo-gravimetric analysis and gamma spectroscopy. The *in-vitro* radiolabeling efficiency was also tested in both 0.9% sodium chloride solution and human blood plasma over a duration of 550 h.

Research results
The SmAcAc-PLLA microspheres with different SmAcAc contents remained spherical before and after neutron activation. The mean diameter of the microspheres was about 35 μm. Specific activity achieved for ^{153}SmAcAc-PLLA microspheres with 100%, 150%, 175% and 200% (w/w) SmAcAc after 3 h neutron activation were 1.7 ± 0.05, 2.5 ± 0.05, 2.7 ± 0.07 and 2.8 ± 0.09 GBq/g, respectively. The activity of per microspheres were determined as 48.36 ± 1.33, 74.10 ± 1.65, 97.87 ± 2.48 and 109.83 ± 3.71 Bq for ^{153}SmAcAc-PLLA microspheres with 100%, 150%, 175% and 200% (w/w) SmAcAc. The energy dispersive X-ray and gamma spectrometry showed that no elemental and radioactive impurities present in the microspheres after neutron activation. Retention efficiency of 153Sm in the SmAcAc-PLLA microspheres was excellent (about 99%) in both 0.9% sodium chloride solution and human blood plasma over a duration of 550 h.

Research conclusions
The ^{153}SmAcAc-PLLA microsphere is potentially useful for hepatic radioembolization due to their biodegradability, favorable physicochemical characteristics and excellent radiolabeling efficiency. The synthesis of the formulation does not involve ionizing radiation and hence reducing the complication and cost of production.

Research perspectives
A neutron-activated, biodegradable ^{153}SmAcAc-PLLA microspheres formulation has been developed and tested for radioembolization of hepatic tumors. Further studies are needed to complete the dosimetry and to compare the radioembolization efficiency with the commercially available formulations.

ACKNOWLEDGEMENTS
The neutron activation was supported by the Malaysian Nuclear Agency.

REFERENCES
1 **Bray F**, Ferlay J, Soerjomataram I, Siegel RL, Torre LA, Jemal A. Global cancer statistics 2018: GLOBOCAN estimates of incidence and mortality worldwide for 36 cancers in 185 countries. *CA Cancer J Clin* 2018; **68**: 394-424 [PMID: 30207593 DOI: 10.3322/caac.21492]
2 **Ferlay J**, Soerjomataram I, Dikshit R, Eser S, Mathers C, Rebelo M, Parkin DM, Forman D, Bray F. Cancer incidence and mortality worldwide: sources, methods and major patterns in GLOBOCAN 2012. *Int J Cancer* 2015; **136**: E359-E386 [PMID: 25220842 DOI: 10.1002/ijc.29210]
3 **Kelly CM**, Kemeny NE. Liver-directed therapy in metastatic colorectal cancer. *Expert Rev Anticancer Ther* 2017; **17**: 745-758 [PMID: 28636427 DOI: 10.1080/14737140.2017.1345629]
4 **Bruix J**, Sherman M; Practice Guidelines Committee, American Association for the Study of Liver Diseases. Management of hepatocellular carcinoma. *Hepatology* 2005; **42**: 1208-1236 [PMID: 16250051 DOI: 10.1002/hep.20933]
5 **Bruix J**, Reig M, Sherman M. Evidence-Based Diagnosis, Staging, and Treatment of Patients With Hepatocellular Carcinoma. *Gastroenterology* 2016; **150**: 835-853 [PMID: 26795574 DOI: 10.1053/j.gastro.2015.12.041]
6 **Mathurin P**, Rixe O, Carbonell N, Bernard B, Cluzel P, Bellin MF, Khayat D, Opolon P, Poynard T. Review article: Overview of medical treatments in unresectable hepatocellular carcinoma--an impossible meta-analysis? *Aliment Pharmacol Ther* 1998; **12**: 111-126 [PMID: 9692685 DOI: 10.1046/j.1365-2036.1998.00286.x]
7 **Lambert B**, Van de Wiele C. Treatment of hepatocellular carcinoma by means of radiopharmaceuticals. *Eur J Nucl Med Mol Imaging* 2005; **32**: 980-989 [PMID: 16032439 DOI: 10.1007/s00259-005-1859-z]
8 **Van Hazel G**, Blackwell A, Anderson J, Price D, Moroz P, Bower G, Cardaci G, Gray B. Randomised phase 2 trial of SIR-Spheres plus fluorouracil/leucovorin chemotherapy versus fluorouracil/leucovorin chemotherapy alone in advanced colorectal cancer. *J Surg Oncol* 2004; **88**: 78-85 [PMID: 15499601 DOI: 10.1002/jso.20141]
9 **Burton MA**, Gray BN, Klemp PF, Kelleher DK, Hardy N. Selective internal radiation therapy: distribution

of radiation in the liver. *Eur J Cancer Clin Oncol* 1989; **25**: 1487-1491 [PMID: 2591440 DOI: 10.7861/clinmedicine.17-5-449]
10 **Ackerman NB**, Lien WM, Kondi ES, Silverman NA. The blood supply of experimental liver metastases. I. The distribution of hepatic artery and portal vein blood to "small" and "large" tumors. *Surgery* 1969; **66**: 1067-1072 [PMID: 5402533]
11 **Hoefnagel CA**. Radionuclide therapy revisited. *Eur J Nucl Med* 1991; **18**: 408-431 [PMID: 1879447 DOI: 10.1007/bf02258432]
12 **Kennedy AS**, McNeillie P, Dezarn WA, Nutting C, Sangro B, Wertman D, Garafalo M, Liu D, Coldwell D, Savin M, Jakobs T, Rose S, Warner R, Carter D, Sapareto S, Nag S, Gulec S, Calkins A, Gates VL, Salem R. Treatment parameters and outcome in 680 treatments of internal radiation with resin 90Y-microspheres for unresectable hepatic tumors. *Int J Radiat Oncol Biol Phys* 2009; **74**: 1494-1500 [PMID: 19157721 DOI: 10.1016/j.ijrobp.2008.10.005]
13 **Kennedy A**, Nag S, Salem R, Murthy R, McEwan AJ, Nutting C, Benson A, Espat J, Bilbao JI, Sharma RA, Thomas JP, Coldwell D. Recommendations for radioembolization of hepatic malignancies using yttrium-90 microsphere brachytherapy: a consensus panel report from the radioembolization brachytherapy oncology consortium. *Int J Radiat Oncol Biol Phys* 2007; **68**: 13-23 [PMID: 17448867 DOI: 10.1016/j.ijrobp.2006.11.060]
14 **Salem R**, Lewandowski RJ. Chemoembolization and radioembolization for hepatocellular carcinoma. *Clin Gastroenterol Hepatol* 2013; **11**: 604-11; quiz e43-44 [PMID: 23357493 DOI: 10.1016/j.cgh.2012.12.039]
15 **Pasciak AS**, Bourgeois AC, Bradley YC. A Microdosimetric Analysis of Absorbed Dose to Tumor as a Function of Number of Microspheres per Unit Volume in 90Y Radioembolization. *J Nucl Med* 2016; **57**: 1020-1026 [PMID: 26912424 DOI: 10.2967/jnumed.115.163444]
16 **Hossain KMZ**, Patel U, Ahmed I. Development of microspheres for biomedical applications: a review. *Prog Biomater* 2015; **4**: 1-19 [PMID: 29470791 DOI: 10.1007/s40204-014-0033-8]
17 **Elschot M**, Nijsen JF, Dam AJ, de Jong HW. Quantitative evaluation of scintillation camera imaging characteristics of isotopes used in liver radioembolization. *PLoS One* 2011; **6**: e26174 [PMID: 22073149 DOI: 10.1371/journal.pone.0026174]
18 **Chakravarty R**, Dash A, Pillai MR. Availability of yttrium-90 from strontium-90: a nuclear medicine perspective. *Cancer Biother Radiopharm* 2012; **27**: 621-641 [PMID: 23009585 DOI: 10.1089/cbr.2012.1285]
19 **Yeong CH**, Abdullah BJ, Ng KH, Chung LY, Goh KL, Sarji SA, Perkins AC. Neutron-activated ^{13}Sm-ion-exchange resin as a tracer for gastrointestinal scintigraphy. *Nucl Med Commun* 2011; **32**: 1256-1260 [PMID: 21934547 DOI: 10.1097/MNM.0b013e32834b3ac8]
20 **Yeong CH**, Abdullah BJ, Ng KH, Chung LY, Goh KL, Sarji SA, Perkins AC. Production and first use of 153SmCl3-ion exchange resin capsule formulation for assessing gastrointestinal motility. *Appl Radiat Isot* 2012; **70**: 450-455 [PMID: 22178699 DOI: 10.1016/j.apradiso.2011.11.056]
21 **Yeong CH**, Abdullah BJ, Ng KH, Chung LY, Goh KL, Perkins AC. Fusion of gamma scintigraphic and magnetic resonance images improves the anatomical delineation of radiotracer for the assessment of gastrointestinal transit. *Nucl Med Commun* 2013; **34**: 645-651 [PMID: 23612704 DOI: 10.1097/MNM.0b013e32836141e4]
22 **Wong YH**, Tan HY, Kasbollah A, Abdullah BJJ, Shah MNM, Yeong CH. Biodegradable Samarium-153–labelled microspheres for hepatic radioembolization: preparation, characterization and radiolabelling evaluation after neutron activation. *Journal of Physics: Conference Series* 2019; **1248**: 012066 [DOI: 10.1088/1742-6596/1248/1/012066]
23 **Babich IV**, Plyuto YV, Van Langeveld AD, Moulijn JA. Role of the support nature in chemisorption of Ni(acac)2 on the surface of silica and alumina. *Appl Surf Sci* 1997; **3**: 267-272 [DOI: 10.1016/S0169-4332(96)01016-1]
24 **Dunstan PO**. Thermochemistry of adducts of nickel(II) acetylacetonate chelate with heterocyclic bases. *Thermochim Acta* 1998; **2**: 165-174 [DOI: 10.1016/S0040-6031(98)00382-7]
25 **Dunstan PO**. Thermochemistry of aniline-derivative adducts of nickel(II) acetylacetonate. *Thermochim Acta* 1999; **1**: 5-11 [DOI: 10.1016/S0040-6031(99)00084-2]
26 **Kennedy A**. Radioembolization of hepatic tumors. *J Gastrointest Oncol* 2014; **5**: 178-189 [PMID: 24982766 DOI: 10.3978/j.issn.2078-6891.2014.037]
27 **Tsai CL**, Chung HT, Chu W, Cheng JCH. Radiation therapy for primary and metastatic tumors of the liver. *J Radiat Oncol* 2012; **3**: 227-237 [DOI: 10.1007/s13566-012-0045-8]
28 **Mumper RJ**, Ryo UY, Jay M. Neutron-activated holmium-166-poly (L-lactic acid) microspheres: a potential agent for the internal radiation therapy of hepatic tumors. *J Nucl Med* 1991; **32**: 2139-2143 [PMID: 1941151]
29 **Poorbaygi H**, Reza Aghamiri SM, Sheibani S, Kamali-Asl A, Mohagheghpoor E. Production of glass microspheres comprising 90Y and (177)Lu for treating of hepatic tumors with SPECT imaging capabilities. *Appl Radiat Isot* 2011; **69**: 1407-1414 [PMID: 21723135 DOI: 10.1016/j.apradiso.2011.05.026]
30 **Häfeli UO**, Roberts WK, Pauer GJ, Kraeft SK, Macklis RM. Stability of biodegradable radioactive rhenium (Re-186 and Re-188) microspheres after neutron-activation. *Appl Radiat Isot* 2001; **54**: 869-879 [PMID: 11300399 DOI: 10.1016/s0969-8043(00)00313-4]
31 **Hashikin NA**, Yeong CH, Abdullah BJ, Ng KH, Chung LY, Dahalan R, Perkins AC. Neutron Activated Samarium-153 Microparticles for Transarterial Radioembolization of Liver Tumour with Post-Procedure Imaging Capabilities. *PLoS One* 2015; **10**: e0138106 [PMID: 26382059 DOI: 10.1371/journal.pone.0138106]
32 **Nijsen JF**, Zonnenberg BA, Woittiez JR, Rook DW, Swildens-van Woudenberg IA, van Rijk PP, van het Schip AD. Holmium-166 poly lactic acid microspheres applicable for intra-arterial radionuclide therapy of hepatic malignancies: effects of preparation and neutron activation techniques. *Eur J Nucl Med* 1999; **26**: 699-704 [PMID: 10398817 DOI: 10.1007/s002590050440]
33 **Lampe KJ**, Namba RM, Silverman TR, Bjugstad KB, Mahoney MJ. Impact of lactic acid on cell proliferation and free radical-induced cell death in monolayer cultures of neural precursor cells. *Biotechnol Bioeng* 2009; **103**: 1214-1223 [PMID: 19408314 DOI: 10.1002/bit.22352]
34 **Mumper RJ**, Jay M. Formation and stability of lanthanide complexes and their encapsulation into polymeric microspheres. *J Phys Chem* 1992; **21**: 8626-8631 [DOI: 10.1021/j100200a076]
35 **Subedi G**, Shrestha AK, Shakya S. Study of effect of different factors in formulation of micro and nanospheres with solvent evaporation technique. *Open Pharmaceutical Sciences Journal* 2016; **3**: 182 [DOI: 10.2174/1874844901603010182]

36 **Dormandy JA**. Clinical significance of blood viscosity. *Ann R Coll Surg Engl* 1970; **47**: 211-228 [PMID: 5475693]
37 **Häfeli UO**, Casillas S, Dietz DW, Pauer GJ, Rybicki LA, Conzone SD, Day DE. Hepatic tumor radioembolization in a rat model using radioactive rhenium (186Re/188Re) glass microspheres. *Int J Radiat Oncol Biol Phys* 1999; **44**: 189-199 [PMID: 10219814 DOI: 10.1016/s0360-3016(98)00554-9]
38 **International Atomic Energy Agency 2019**. Research Reactor Database (RRDB) [Internet]. [cited 2019 Jul 28]. Available from: https://nucleus.iaea.org/RRDB/RR/ReactorSearch.aspx?rf=1

Published By Baishideng Publishing Group Inc
7041 Koll Center Parkway, Suite 160, Pleasanton, CA 94566, USA
Telephone: +1-925-3991568
E-mail: bpgoffice@wjgnet.com
Help Desk: https://www.f6publishing.com/helpdesk
https://www.wjgnet.com

© 2020 Baishideng Publishing Group Inc. All rights reserved.

ISSN 2220-315x (online)

World Journal of *Experimental Medicine*

World J Exp Med 2020 April 27; 10(3): 26-40



Published by Baishideng Publishing Group Inc

World Journal of Experimental Medicine

Contents

Irregular Volume 10 Number 3 April 27, 2020

ORIGINAL ARTICLE

Basic Study

26 Isolation and identification of adipose-derived stromal/stem cells from breast cancer patients after exposure neoadjuvant chemotherapy
Hagaman AR, Zhang P, Koko KR, Nolan RS, Fromer MW, Gaughan J, Matthews M

Contents

World Journal of Experimental Medicine

Volume 10 Number 3 April 27, 2020

ABOUT COVER

Editorial Board Member of *World Journal of Experimental Medicine*, Mikhail Alexeyev, PhD, Associate Professor, Department of Cell Biology and Neuroscience, University of South Alabama, Mobile, AL 36688, United States

AIMS AND SCOPE

The primary aim of the *World Journal of Experimental Medicine* (*WJEM*, *World J Exp Med*) is to provide scholars and readers from various fields of experimental medicine with a platform to publish high-quality basic and clinical research articles and communicate their research findings online.

WJEM mainly publishes articles reporting research results and findings obtained in the field of experimental medicine and covering a wide range of topics including clinical laboratory medicine (applied and basic research in hematology, body fluid examination, cytomorphology, genetic diagnosis of hematological disorders, thrombosis and hemostasis, and blood typing and transfusion), biochemical examination (applied and basic research in laboratory automation and information system, biochemical methodology, and biochemical diagnostics), *etc*.

INDEXING/ABSTRACTING

The *WJEM* is now abstracted and indexed in PubMed, PubMed Central, China National Knowledge Infrastructure (CNKI), and Superstar Journals Database.

RESPONSIBLE EDITORS FOR THIS ISSUE

Responsible Electronic Editor: *Yan-Xia Xing*

Proofing Production Department Director: *Yun-Xiaojian Wu*

Responsible Editorial Office Director: *Jia-Ping Yan*

NAME OF JOURNAL
World Journal of Experimental Medicine

ISSN
ISSN 2220-315x (online)

LAUNCH DATE
December 20, 2011

FREQUENCY
Irregular

EDITORS-IN-CHIEF
Arnon Blum

EDITORIAL BOARD MEMBERS
https://www.wjgnet.com/2220-315x/editorialboard.htm

PUBLICATION DATE
April 27, 2020

COPYRIGHT
© 2020 Baishideng Publishing Group Inc

INSTRUCTIONS TO AUTHORS
https://www.wjgnet.com/bpg/gerinfo/204

GUIDELINES FOR ETHICS DOCUMENTS
https://www.wjgnet.com/bpg/GerInfo/287

GUIDELINES FOR NON-NATIVE SPEAKERS OF ENGLISH
https://www.wjgnet.com/bpg/gerinfo/240

PUBLICATION ETHICS
https://www.wjgnet.com/bpg/GerInfo/288

PUBLICATION MISCONDUCT
https://www.wjgnet.com/bpg/gerinfo/208

ARTICLE PROCESSING CHARGE
https://www.wjgnet.com/bpg/gerinfo/242

STEPS FOR SUBMITTING MANUSCRIPTS
https://www.wjgnet.com/bpg/GerInfo/239

ONLINE SUBMISSION
https://www.f6publishing.com

© 2020 Baishideng Publishing Group Inc. All rights reserved. 7041 Koll Center Parkway, Suite 160, Pleasanton, CA 94566, USA
E-mail: bpgoffice@wjgnet.com https://www.wjgnet.com

World Journal of Experimental Medicine

Submit a Manuscript: https://www.f6publishing.com

World J Exp Med 2020 April 27; 10(3): 26-40

DOI: 10.5493/wjem.v10.i3.26

ISSN 2220-315x (online)

ORIGINAL ARTICLE

Basic Study

Isolation and identification of adipose-derived stromal/stem cells from breast cancer patients after exposure neoadjuvant chemotherapy

Ashleigh Rapp Hagaman, Ping Zhang, Kiavash R Koko, Ryan S Nolan, Marc W Fromer, John Gaughan, Martha Matthews

ORCID number: Ashleigh Rapp Hagaman (0000-0003-0567-2984); Ping Zhang (000-0001-6581-7941); Kiavash R Koko (0000-0002-1952-749X); Ryan Nolan (0000-0002-8045-9879); Marc W Fromer (0000-0002-6052-2455); John Gaughan (0000-0001-7798-2047); Martha Matthews (0000-0002-9470-0002).

Author contributions: Hagaman AR and Zhang P performed conception and design, collected samples, the majority of experiments, analyzed the data and wrote the article; Koko KR, Nolan RS and Fromer MW collected samples, clinical analysis, and interpretation; Matthews M performed conception and design, patients selection and collected samples, clinical analysis, and interpretation; Gaughan J, a senior biostatistician performed study statistical analysis.

Institutional review board statement: All patients provided written informed consent in accordance with our IRB-approved protocol by Cooper Health Care Institutional Review Board (Protocol approval number # 15-107EX/2015, name: Examining the potential impact of chemotherapy and radiation on mesenchymal stem cells in cancer patients).

Conflict-of-interest statement: The authors declare that there is no conflict of interest regarding the publication of this paper.

Ashleigh Rapp Hagaman, Ping Zhang, Kiavash R Koko, Ryan S Nolan, Marc W Fromer, John Gaughan, Martha Matthews, Department of Surgery, Cooper University Hospital, Camden, NJ 08103, United States

Ping Zhang, John Gaughan, Martha Matthews, Cooper Medical School of Rowan University, Camden, NJ 08103, United States

Corresponding author: Ping Zhang, DDS, PhD, Assistant Professor, Department of Surgery, Cooper University Hospital, Cooper Medical School of Rowan University, 401 Haddon Avenue, Camden, NJ 08103, United States. zhang-ping@cooperhealth.edu

Abstract

BACKGROUND

With recent research advances, adipose-derived stromal/stem cells (ASCs) have been demonstrated to facilitate the survival of fat grafts and thus are increasingly used for reconstructive procedures following surgery for breast cancer. Unfortunately, in patients, following radiation and chemotherapy for breast cancer suggest that these cancer treatment therapies may limit stem cell cellular functions important for soft tissue wound healing. For clinical translation to patients that have undergone cancer treatment, it is necessary to understand the effects of these therapies on the ASC's ability to improve fat graft survival in clinical practice.

AIM

To investigate whether the impact on ASCs function capacity and recovery in cancer patients may be due to the chemotherapy.

METHODS

ASCs were isolated from the cancerous side and noncancerous side of the breast from the same patients with receiving neoadjuvant chemotherapy (NAC) or not-receiving NAC. ASCs were *in vitro* treated with 5-fluorouracil (5-FU), doxorubicin (DXR), and cyclophosphamide (Cytoxan) at various concentrations. The stem cells yield, cell viability, and proliferation rates were measured by growth curves and MTT assays. Differentiation capacity for adipogenesis was determined by qPCR analysis of the specific gene markers and histological staining.

Data sharing statement: No additional data are available.

Open-Access: This article is an open-access article that was selected by an in-house editor and fully peer-reviewed by external reviewers. It is distributed in accordance with the Creative Commons Attribution NonCommercial (CC BY-NC 4.0) license, which permits others to distribute, remix, adapt, build upon this work non-commercially, and license their derivative works on different terms, provided the original work is properly cited and the use is non-commercial. See: http://creativecommons.org/licenses/by-nc/4.0/

Manuscript source: Invited Manuscript

Received: December 9, 2019
Peer-review started: December 9, 2019
First decision: December 26, 2019
Revised: February 4, 2020
Accepted: March 28, 2020
Article in press: March 28, 2020
Published online: April 27, 2020

P-Reviewer: Kode JA, Leung PC
S-Editor: Gong ZM
L-Editor: A
E-Editor: Li X

RESULTS

No significant differences were observed between the yield of ASCs in patients receiving NAC treatment and not-receiving NAC. ASCs yield from the cancerous side of the breast showed lower than the noncancerous side of the breast in both patients receiving NAC and not-receiving NAC. The proliferation rates of ASCs from patients didn't differ much before and after NAC upon *in vitro* culture, and these cells appeared to retain the capacity to acquire adipocyte traits simile to the ASCs from patients not-receiving NAC. After cessation and washout of the drugs for another a week of culturing, ASCs showed a slow recovery of cell growth capacity in 5-FU-treated groups but was not observed in ASCs treated with DXR groups.

CONCLUSION

Neoadjuvant therapies do not affect the functioning capacity of ASCs. ASCs may hold great potential to serve as a cell source for fat grafting and reconstruction in patients undergoing chemotherapy.

Key words: Human adipose-derived stromal/stem cells; Breast cancer; Neoadjuvant chemotherapy; Chemotherapeutic agents; Adipogenic differentiation; Proliferation

©The Author(s) 2020. Published by Baishideng Publishing Group Inc. All rights reserved.

Core tip: The functioning capacity and recovery potential of adipose-derived mesenchymal stromal/stem cells (ASCs) were demonstrated in terms of the stem cell yield, proliferation rates and adipogenic differentiation capabilities in breast cancer patients after exposure to neoadjuvant therapies (NAC) treatment. The yield of ASCs did not alter much after NAC treatment of patients. Moreover, the proliferation rates of ASCs derived from patients didn't differ much before and after NAC upon *in vitro* culture, and these cells appeared to retain the differentiation capacity to acquire adipocyte traits simile to those ASC obtained from the patients not-receiving NAC.

Citation: Hagaman AR, Zhang P, Koko KR, Nolan RS, Fromer MW, Gaughan J, Matthews M. Isolation and identification of adipose-derived stromal/stem cells from breast cancer patients after exposure neoadjuvant chemotherapy. *World J Exp Med* 2020; 10(3): 26-40
URL: https://www.wjgnet.com/2220-315x/full/v10/i3/26.htm
DOI: https://dx.doi.org/10.5493/wjem.v10.i3.26

INTRODUCTION

Breast cancer is a leading cause of death in women with approximately 1.7 million new cases and over 522000 deaths per year[1]. However, the overall number of breast reconstructions has lately considerably increased, currently, there are about 93000 breast reconstructions performed in the United States per year[2,3]. Breast reconstruction including implant-and expander-based breast reconstruction, and nowadays, autologous fat grafting (non-vascularized autologous lipoaspirate fat) is being increasingly used for reconstructive procedures following surgery for breast cancer patients[4-6]. With recent research advances, cell-assisted lipotransfer studies concluded that it was more efficacious than autologous fat grafting alone, and adipose-derived mesenchymal stromal/stem cells (ASCs) have been demonstrated to facilitate the survival of fat grafts and thus increasingly used for reconstructive procedures following surgery for breast cancer[7,8]. ASCs, as an abundant source of adult mesenchymal stem cells, easily harvested, possess multiple characteristics that make them ideal for regenerative and complementary medicine applications[9,10]. Unfortunately, the problem of poor soft tissue wound healing in cancer patients post-exposure to radiation and chemotherapy suggests that these cancer treatment therapies may limit ASC cellular functions important for soft tissue wound healing[11-13]. Our previous *in vitro* human data demonstrates that direct exposure to chemotherapeutic agents (tamoxifen and paclitaxel) has a cytotoxic effect by decreasing ASCs proliferation rates and multi-potency differentiating abilities[13-15]. However, we have yet to examine the effects of chemotherapy on ASCs outcomes in patients. Importantly, for clinical translation to patients that have undergone radiation

and/or chemotherapy, it is necessary to better understand the effects of these therapies on the ASC ability to improve fat graft survival in clinical practice. In addition, recent research has focused almost entirely on poor soft tissue wound healing in patients exposure to radiation/or chemotherapy, but little is known about the recovery of cell viability and function capability of stem cells in patients after chemotherapeutic-treatment[16]. Accordingly, this study aimed to determine the effects of chemotherapy on ASCs by examining human breast tissue specimens from cancer patients receiving neoadjuvant therapies (NAC) treatment and compared to the patients not-receiving NAC regarding their yield, proliferation capacity, and especially their potency to differentiate into a functional adipocyte-phenotype to clarify whether the impact on ASC function and recovery capacities may be due to the chemotherapy.

Autologous fat grafting (lipofilling) for breast reconstruction after surgery is performed frequently, investigations studying the functional capability and recovery of stem cells in tumor environment with chemotherapy treatment have been inadequate[17,18]. In the presents study, we involved a comparison study to analysis of the stem cells yield, proliferative and adipogenesis differentiation capacities of ASCs from the cancerous side of the breast and noncancerous side of the breast from the same patient who underwent scheduled bilateral mastectomies with reconstruction at the time of resection about 6-8 wk receiving neoadjuvant chemotherapy and compared with the patients who have not-receiving NAC.

Furthermore, nowadays, neoadjuvant therapy has become increasingly common for many patients, as this is associated with reduced recurrence rates and mortality[19]. According to the National Comprehensive Cancer Network, there are several combinations of neoadjuvant therapies including cytotoxic, endocrine, and biologic target agents for the treatment of breast cancer[20,21]. Herein, the second aim of this study was to investigate, *in vitro*, the cellular functions of ASCs after exposure to three commonly utilized clinical chemotherapeutic agents: 5-fluorouracil (5-FU), doxorubicin (DXR), and cyclophosphamide (Cytoxan) to determine whether the ASCs viability diminished in the presence of these agents commonly used neoadjuvant chemotherapies, or patterns of recovery after cessation of these chemotherapeutic drugs in treatment. The results of our study will provide important information and further understanding regarding the use of autologous ASCs in reconstructive procedures following chemotherapy such as in breast cancer patients.

MATERIALS AND METHODS

Patient selection

Breast cancer patients who underwent scheduled bilateral mastectomies with reconstruction included in this study (n = 21). All patients provided written informed consent following our institutional review board-approved protocol. Patients were included if they were 18 years and older, getting bilateral resection with reconstruction, and had a diagnosis of breast cancer on one side. Patients were excluded if they had bilateral premalignant and/or malignant lesions, had a unilateral prophylactic mastectomy, or if they were less than 18 years old. The demographic and clinical characteristics of all patients have summarized in Table 1. ASCs were isolated from the cancerous side and noncancerous side of the breast from the same patient who underwent scheduled bilateral mastectomies with reconstruction at the time of resection about 6-8 weeks receiving NAC treatment or not-receiving NAC regarding their yield, proliferation rates, and especially their potency to differentiate into a functional adipocyte-phenotype (Figure 1).

Human tissue collection and ASCs isolation

Adipose tissue specimens were collected from the cancerous side of the breast and noncancerous side of the breast from the same patient receiving NAC treatment or not-receiving NAC. Adipose tissue was washed with phosphate-buffered saline (PBS) and the isolation of ASCs was performed as previously described[22]. Adipose tissue was incubated for 1 h at 37 °C with collagenase I solution (Worthington) with shaking. After centrifugation (1500 rpm/10 min), the stromal vascular fraction (SVF) was cultured in basal medium 199 (Mediatech; Manassas, VA) supplemented with 10% fetal bovine serum (Gemini Bio Products; West Sacramento, CA). After 24 h incubation, the media was aspirated to remove any unattached cells and washed with PBS; complete culture media was subsequently replaced twice weekly.

Proliferation assays

The primary isolated ASCs from patients receiving NAC or not-receiving NAC were

Table 1 Clinical and pathological characteristics of the experimental population, *n* (%)

Patient demographics	No neoadjuvant chemotherapy, *n* = 10	Neoadjuvant chemotherapy, *n* = 11	*P* value
Age, yr	49 ± 6	49 ± 7	1.000
Stage of cancer			
0	2 (9.5)	0 (0)	0.2143
IA	6 (28.5)	2 (9.5)	0.0805
IIA	1 (5)	4 (19)	0.3108
IIB	1 (5)	2 (9.5)	1.000
IIIA	0 (0)	3 (14)	0.2143
Menopausal	4 (19)	5 (24)	1.000
Multiparous	10 (48)	9 (43)	0.4762
ER+	9 (43)	8 (38)	0.5865
PR+	10 (48)	5 (24)	0.0124
Her2+	3 (14)	6 (28.5)	0.3870
Tobacco	3 (14)	1 (5)	0.3108

submitted for proliferation and differentiation experimentation at passages 3–5. Proliferation rates were assessed by constructing growth curves during 11-d periods. ASCs were plated at 2.5 × 10^3 cells/cm^2 and fed every other day. At various time points, cells were trypsin-released and counted with a Coulter counter (Beckman Coulter, Inc., Fullerton, CA, United States).

Adipogenic differentiation of ASCs

To evaluate the adipogenic differentiation capacity of ASCs, ASCs from patients receiving NAC or not-receiving NAC were cultured in AdipoDiff Medium (Gbico Life Technologies) for three weeks. Commitment toward an adipocyte lineage was measured by evaluating mRNA expression of the adipocyte markers of lipoprotein lipase (LPL) and peroxisome proliferator activated receptor gamma (PPAR-γ) by quantitative PCR, and histological Oil red O staining. The differentiated ASCs were incubated with cooled methanol for 5 min and stained with fresh Oil Red-O (Sigma-Aldrich) solution for 20 min then the photomicrographs were taken to identify lipid droplets. In addition, the adipogenic differentiation levels of ASCs were quantified by extracting the oil red O dye with 100% isopropanol and using optical density readings taken at a wavelength of 495 nm (100% isopropanol as a background).

Quantitative real-time polymerase chain reaction

Total RNA was extracted using TRIzol (Life technologies; Grand Island, NY, United States) reagent. To detect the specific genes expressed in adipogenic differentiated ASCs, RT-PCR was performed using the following primers: Peroxisome proliferator-activated receptor gamma (PPAR-γ) with 5′-primers (5′-GCTTTTGGCATACTCTG TGATCTC-3′) and 3′-primers (5′-TCAGGGCTGCCAGTTTCG-3′); and Lipoprotein lipase (LPL) with 5-primers (5′-GCTCGTGGGAGCACTTCACT-3′) and 3′-primers (5′-TCCGCGTGATTGCAGAGA-3′). mRNA levels were quantified using SYBR Green Real-Time PCR with the 7500 Fast Real-Time PCR system (Applied Biosystems). PCR reaction conditions were 95 °C for 10 min, followed by 40 cycles of 95 °C for 15 s and 60 °C for 1 min. The housekeeping gene GAPDH (5′-primers: 5′-GGATCTCGCTCC TGGAAGATG-3′) and 3′-primers: 5′-GCACCGTCAAGGCTGAGAAC-3′) were amplified in separate tubes to normalize for variance in input RNA. For relative quantification, the efficiency of amplification for each primer pair was determined using the cDNA target and the $2^{-\Delta\Delta}$ct method.

In vitro treatment of individual chemotherapeutic agents and cell viability assays

For evaluation of the cellular function and recovery potential of ASCs after exposure to chemotherapeutic agents, ASCs isolated from female patients during reconstructive procedures were treated with 5-FU, DXR, and Cytoxan to determine whether the ASC viability diminished in the presence of these three commonly utilized clinical chemotherapeutic agents. 5-FU, DXR, and Cytoxan (Sigma-Aldrich) was dissolved to make a stock concentration solution, aliquoted and kept in -20 °C refrigerator for freshly using each time. ASCs were plated at a density of 1 × 10^4 cells per well in a volume of 1ml in 24 well plates and then treated with 5-FU (0.1, 1, and 10 mg/mL), DXR (0.1, 1, and 10 μmol/L), and Cytoxan (0.1, 1, and 10 mmol/L) at the various concentrations. At 24, 48, and 72 h, MTT assay (3-(4, 5-dimethylthiazol-2-yl)-2, 5-

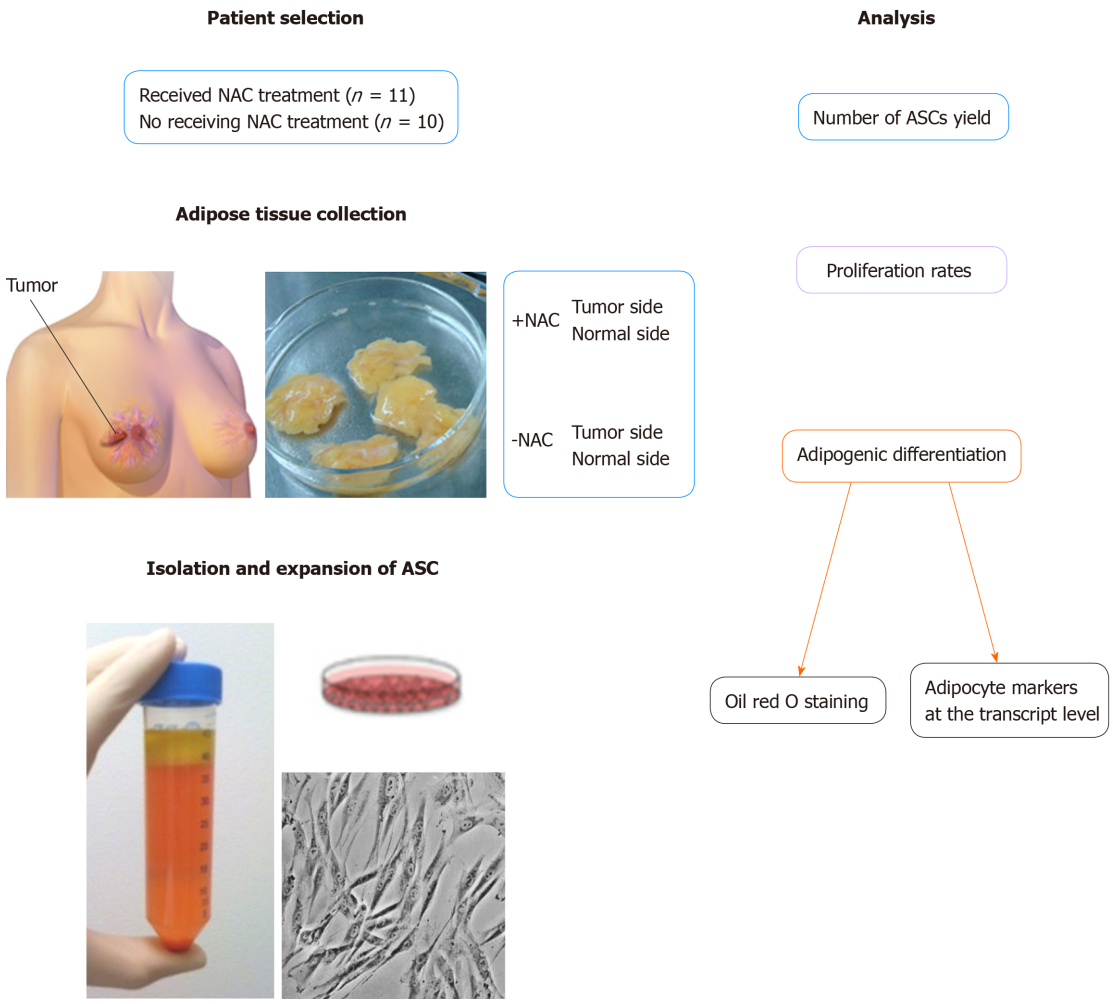


Figure 1 Experimental design. Adipose-derived stromal cells (ASCs) were isolated from both the cancerous side and noncancerous side of the breast from the same patients with receiving neoadjuvant chemotherapy (NAC) treatment or not-receiving NAC. The number of ASCs yield, proliferation rates and the ability to undergo adipogenic differentiation was analyzed by constructing growth curves, quantitative RT-PCR and histological staining and compared to the ASCs obtained from patients not-receiving NAC treatment. ASCs: Adipose-derived stromal cells; NAC: Neoadjuvant chemotherapy.

diphenyl-tetrazolium bromide) was used to evaluate the effect of 5-FU, DXR, and Cytoxan on ASCs cell viabilities. At various time points, the culture medium was replaced with a medium containing MTT solution (5 mg/mL) and incubate at 37 °C with 5% CO_2 for 3 h. The wells were then decanted and the purple formazan crystals formed were dissolved in 200 μL dimethyl sulfoxide solution (Sigma-Aldrich). The absorbance of the plate was read on a microplate reader at 570 nm. Fresh cells were used as controls. All assays were done in triplicate.

ASC proliferation and differentiation with individual chemotherapeutic agents

To evaluate the potential of cellular function recovery of ASCs after treated with the chemotherapeutic agents, we extended the cell culture period. ASCs were plated into 24 well plates at 5 × 10^3 cells /cm^2 and exposure to 5-FU (0.1 or 1 mg/mL) or DXR (0.1 or 1 μmol) for 72 h then the drugs have removed. The cells were cultured in medium without the drug for an additional 8 d, and the proliferation rates were assessed by constructing growth curves for 11 d. At different time points, cells were trypsin released and counted with a coulter counter (Beckman Coulter, Inc, Fullerton, Calif).

To evaluate the multipotency differentiation with these chemotherapeutic agents, ASCs were cultured in AdipoDiff Medium with or without 5-FU (1 mg), DXR (1 μmol/L) and Cytoxan (1 mmol) for three weeks. For osteogenic differentiation, ASC cells were cultured in OsteoDiff Medium (Gibco LifeTechnologies) with or without above chemo-drugs for 3 wk; the cells were then stained with Alizarin Red S solution for 20 min to identify calcium deposits.

Statistical analysis

Cell counts were analyzed as continuous variables and are presented as means with standard deviations. Categorical variables are presented as frequencies with percent.

Group differences of cell counts were analyzed using analysis of variance for repeated measures with follow-up pair-wise comparisons. The count data were tested for normality using the Shapiro Wilk test. In order to use parametric methods on non-normal data, the counts were transformed to normalized ranks prior to analysis. A P value of 0.05 was regarded as being statistically significant. All data were analyzed using SAS v9.4 (SAS Institute, Cary, NC, United States).

RESULTS

Patient characteristics

Human breast adipose tissue specimens were collected from a breast cancer patient's cancerous side of the breast and noncancerous side of the breast in same patients who underwent scheduled bilateral mastectomies with reconstruction at the time of resection about 6-8 wk receiving NAC treatment or not-receiving NAC (age: 31-59 years, n = 21). Table 1 describes the characteristics of the experimental population. The stage of cancer including zero, IA, IIA, IIB, and IIIA patients, and as known with 43% ER and 48% PR positive.

Isolation of ASCs from breast tissue in cancer patients after exposure to NAC treatment

To determine the influence of NAC treatment on stem cell yield, ASCs were isolated from breast cancer patients with receiving NAC treatment or not-receiving NAC. In addition, we have compared the numbers of ASCs yield from the cancerous side of the breast and noncancerous side of the breast from the same patient. As shown in Figure 2A, we observed that the number of ASCs yield was not shown reduced in patients receiving NAC treatment when compared to patients not-receiving NAC from either the cancerous side of the breast (CA-ASC, 0.69 ± 0.20 million/g *vs* 0.52 ± 0.10 million/g, P = 0.46) or noncancerous side of the breast (N-ASC, 0.99 ± 0.29 m million/g *vs* 0.71 ± 0.17 million/g, P = 0.44). However, compared to the noncancerous side of the breast, we found that the numbers of ASCs yield from the cancerous side of breast were lower than the noncancerous side of breast in both patients receiving NAC treatment (30% decreased, P = 0.43) and not-receiving NAC (25% decreased, P = 0.36) (Figure 2B). Furthermore, univariate analysis of the ASCs harvest from the cancerous side of the breast or normal side of the breast adipose failed to reveal any significant correlation between patients receiving NAC and not-receiving NAC (Figure 2C).

ASCs proliferative capacity was not effected in cancer patients after exposure to NAC treatment

We then analysis of the proliferation rates of ASCs from the patients receiving NAC or not-receiving NAC. Compared to the ASCs from patients not-receiving NAC, a trend toward lower proliferation rates was observed in the ASCs that from patients receiving NAC treatment in both that from the cancerous side of the breast (Figure 3A) and noncancerous side of the breast (Figure 3B) as measured by growth curves during 11 d culturing. However, this difference was not shown statistically significantly.

ASCs keep their stem cell differentiation capacity in cancer patients after exposure to NAC treatment

We further analyzed whether in patients receiving NAC treatment affects ASCs adipogenic differentiation capability. ASCs from patients receiving NAC or not-receiving NAC from the patient's cancerous side of breast or noncancerous side of the breast were cultured in adipogenic differentiation medium for three weeks. After three weeks of culture, the ASC has differentiated into the adipocyte phenotype. Oil Red O stain demonstrated that the lipid droplets in the differentiated ASCs that from the patients receiving NAC treatment were similar to the ASCs from patients not-receiving NAC. After extract the Oil red O dye for quantifying the positive adipogenic cells, there was not displayed a significant difference between the ASCs from patients receiving NAC *vs* ASCs from patients not-receiving NAC (Figure 4B). In addition, we have determined the differentiated ASCs expressing the adipocyte markers at the transcript levels. After three weeks of differentiation, qPCR results reveal that ASCs newly expressed the messenger RNA for the adipocyte-specific genes of PPAR-γ and LPL. Compared to the ASCs that from patients not-receiving NAC, we found that there was a trend toward decreased mRNA expression of PPAR-γ and LPL in ASCs that from patients receiving NAC treatment (Figure 4C). However, this difference was also not shown statistically significantly.

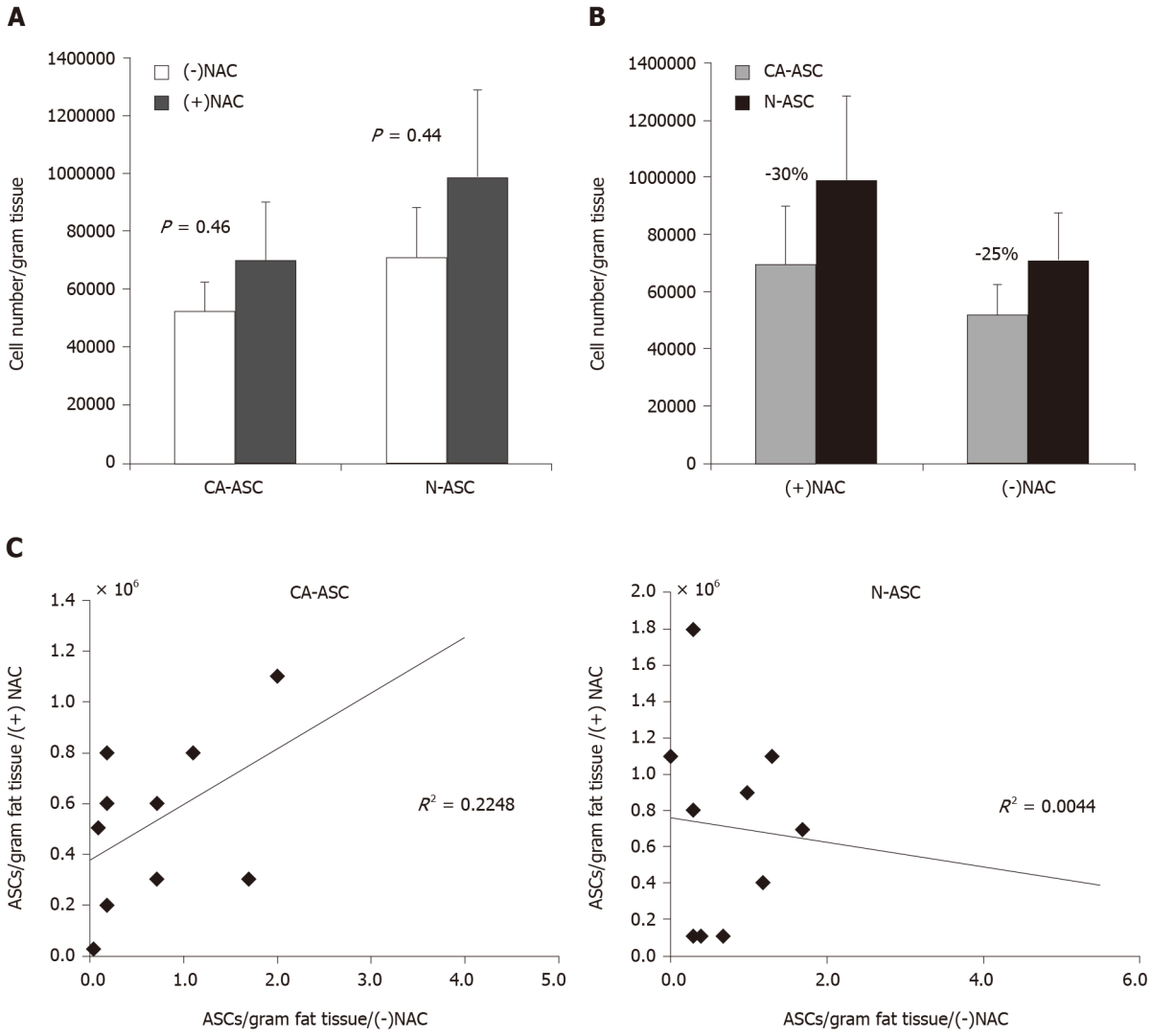


Figure 2 Isolation of adipose-derived stromal cells from breast tissues in patients after received neoadjuvant chemotherapy treatment. A: Number of ASCs isolated per gram of adipose tissue from the cancerous side (CA-ASC) of the breast and noncancerous side (N-ASC) of the breast in patients receiving neoadjuvant chemotherapy (+NAC) *vs* patients not-receiving neoadjuvant chemotherapy (-NAC). B: ASCs yield from the cancerous side of the breast was lower than the noncancerous side of the breast in both patients receiving NAC and not-receiving NAC. C: Overall correlation between the numbers of harvesting ASCs from the cancerous side and noncancerous side of the breast in patients receiving NAC or not-receiving NAC (n = 21, mean ± SE, P = NS). ASCs: Adipose-derived stromal cells; NAC: Neoadjuvant chemotherapy.

Recovery of ASCs viability following exposure to individual chemotherapeutic agents in vitro

To investigate the effects of chemotherapeutic agents on cell viability of ASCs, the cell growth arrest rates were determined at various doses of 5-FU (0.1, 1, and 10 mg/mL), DXR (0.1, 1, and 10 μmol/L), and Cytoxan (0.1, 1, and 10 mmol/L) using MTT assays. In the control group, the cell number increased over the 3-d time course, whereas for ASCs treated with 5-FU and DXR demonstrated decreased growth rates in a dose-dependent and time-dependent manner. However, in ASCs treated with cyclophosphamide groups, the cell viability and growth rates were not shown inhibited when compare to without drug treatment the control groups (Figure 5A). After the withdrawal of the drugs for another 8 d of culturing, in the lower doses of 5-FU treated groups, ASCs showed recovery of the cell's growth capacity which compared to the higher doses of 5-FU treated groups. However, full recovery was not achieved as the numbers of ASCs still significantly lower than the control group (Figure 5B). The recovery of cell viability was not observed in ASCs treated with DXR groups at either low- or high- dose followed by cessation of the drugs for an additional 8 d culturing (approximately 50% decreased *vs* non-treatment control group, $P < 0.05$; Figure 5C).

The adipogenic and osteogenic differentiation capacities of ASCs were decreased in the 5-FU, DXR and Cytoxan treated group when compared with the non-treated control group evidenced by oil red O (Figure 6A) and alizarin red staining (Figure

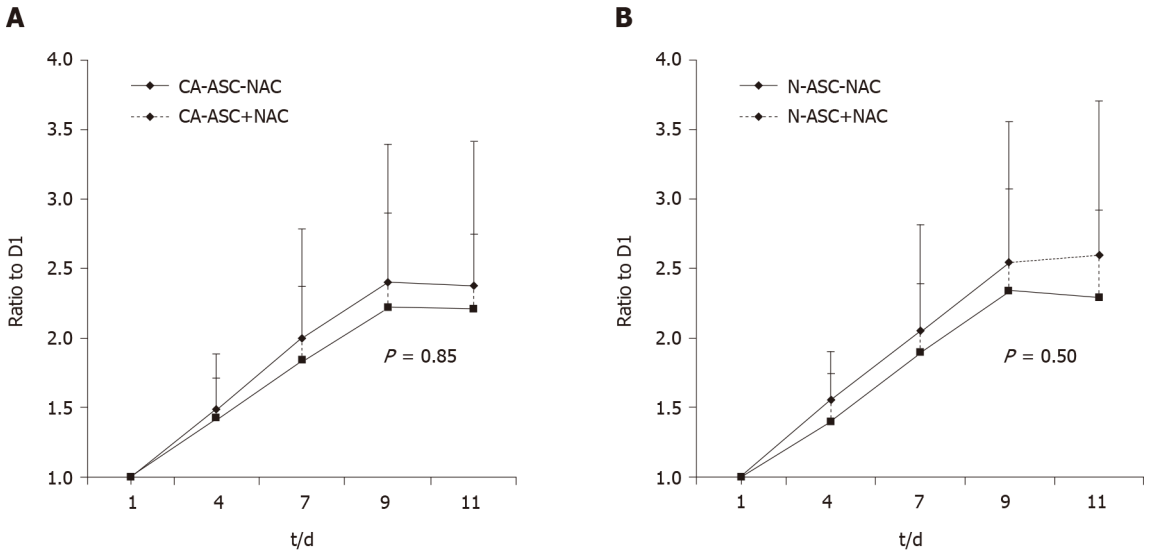


Figure 3 Proliferation of adipose-derived stromal cells in patients after received neoadjuvant chemotherapy treatment. A: Growth curve of ASCs from the cancerous side (CA-ASC) of the breast in patients receiving neoadjuvant chemotherapy (+NAC) *vs* not-receiving neoadjuvant chemotherapy (-NAC) during 11 d culturing. B: Comparison of ASCs from the noncancerous side (N-ASC) of the breast *vs* cancerous side (CA-ASC) of the breast on cell proliferation between patients receiving NAC treatment and not-receiving NAC during 11 d culturing (n = 21, mean ± SE, P = NS). ASC: Adipose-derived stromal cell; NAC: Neoadjuvant chemotherapy.

6B). After extracting the dye from oil red O for positive adipogenic cells and alizarin red for positive osteogenic cells, ASCs displayed the impact of adipogenic (2.1 fold decreased in 5-FU treated group, 2.3 fold in DXR treated group, and 1.3 fold in Cytoxan treated group, $P < 0.05$; Figure 6A) and osteogenic differentiation potential (20 fold decreased in 5-FU treated group, 20 fold in DXR treated group, and 1.5 fold decreased in Cytoxan treated group, $P < 0.05$; Figure 6B).

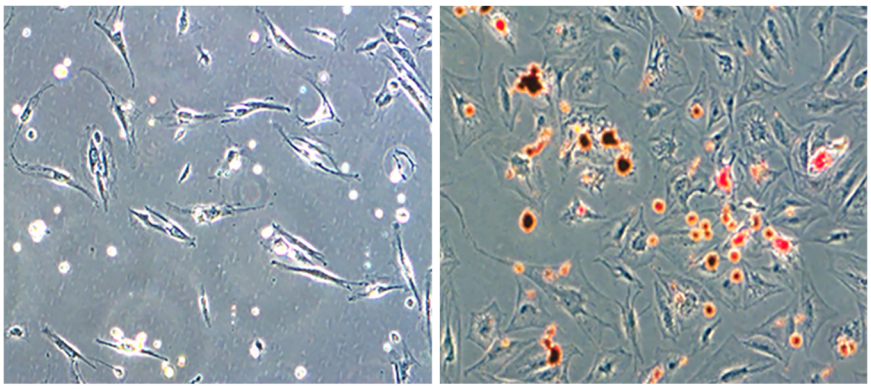
DISCUSSION

Mesenchymal stem/stromal cells are present in many human tissues and organs, in patients post-exposure to cancer treatment therapies may limit their cellular functions important to improve fat graft survival and soft tissue wound healing. In this study, we investigated whether the ASCs have the potential for recovery of the cellular function after exposure to the NAC treatment in breast cancer patients. The major findings of this study include that the yield of ASCs didn't alter much after NAC treatment of patients. Moreover, the proliferation rates of ASCs derived from patients didn't differ much before and after NAC upon *in vitro* culture, and these cells appeared to retain the differentiation capacity to acquire adipocyte traits similar to those ASCs obtained from patients not-receiving NAC. Further, we compared the ability of ASCs derived from the patient's cancerous side of the breast and noncancerous side of the breast in patients receiving NAC or not-receiving NAC. Our study results suggest that ASCs may hold great potential and represents to serve as a cell source for clinical practice in fat grafting and reconstruction in breast cancer patients undergoing chemotherapy treatment.

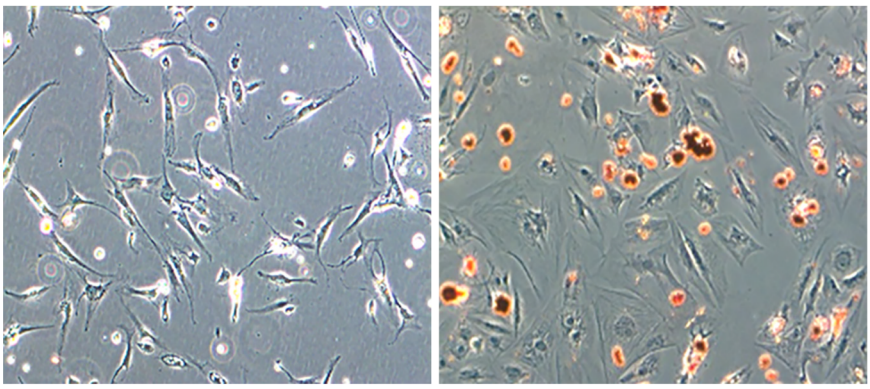
Over the years, stem cell-based therapies have been tested and used in many clinical settings such as outcomes of breast cancer and breast reconstruction[7,23]. In the use of autologous stem cell-based target therapy, an additional challenge is making the cell source readily available for implantation. This study specifically evaluates the availability of ASCs from breast tissue in cancer patients with received NAC treatment. After isolation, we found that there no significant differences were observed between the numbers of ASCs yield in patients receiving NAC treatment with not-receiving NAC and in either from the cancerous side of the breast or noncancerous side of the breast. Of note, we acknowledge that we did not collect the control data that from before starting the treatment in the same patient, we cannot definitively comment upon isolation differences that may exist with this population; nonetheless, the current study demonstrates that ASCs can be isolated in great abundance from the breast adipose tissue in cancer patients after post chemotherapy. In addition, it is of great interest to know we recently described that the ASC can be isolated from the breast smaller fat specimens (approximately 5 g), and expansion to

A

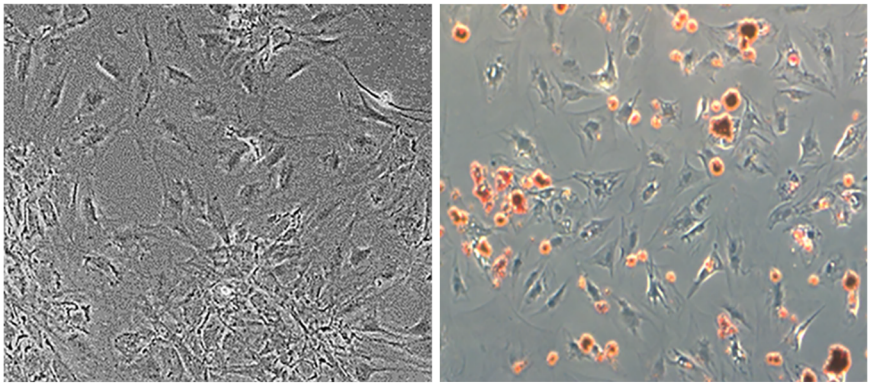
N-ASC/-NAC



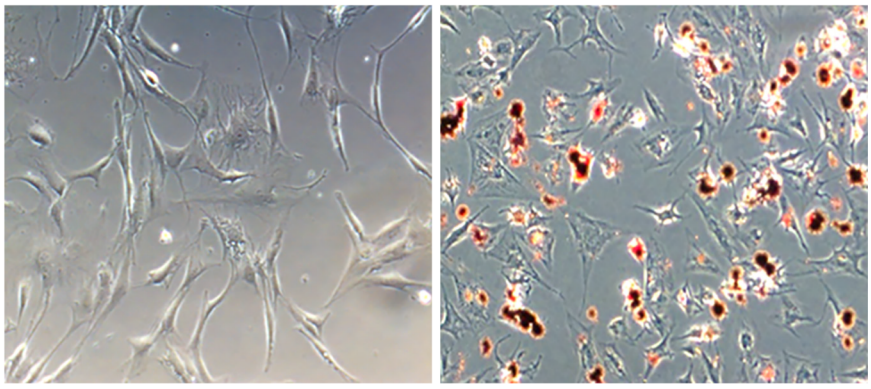
CA-ASC/-NAC



N-ASC/+NAC



CA-ASC/+NAC



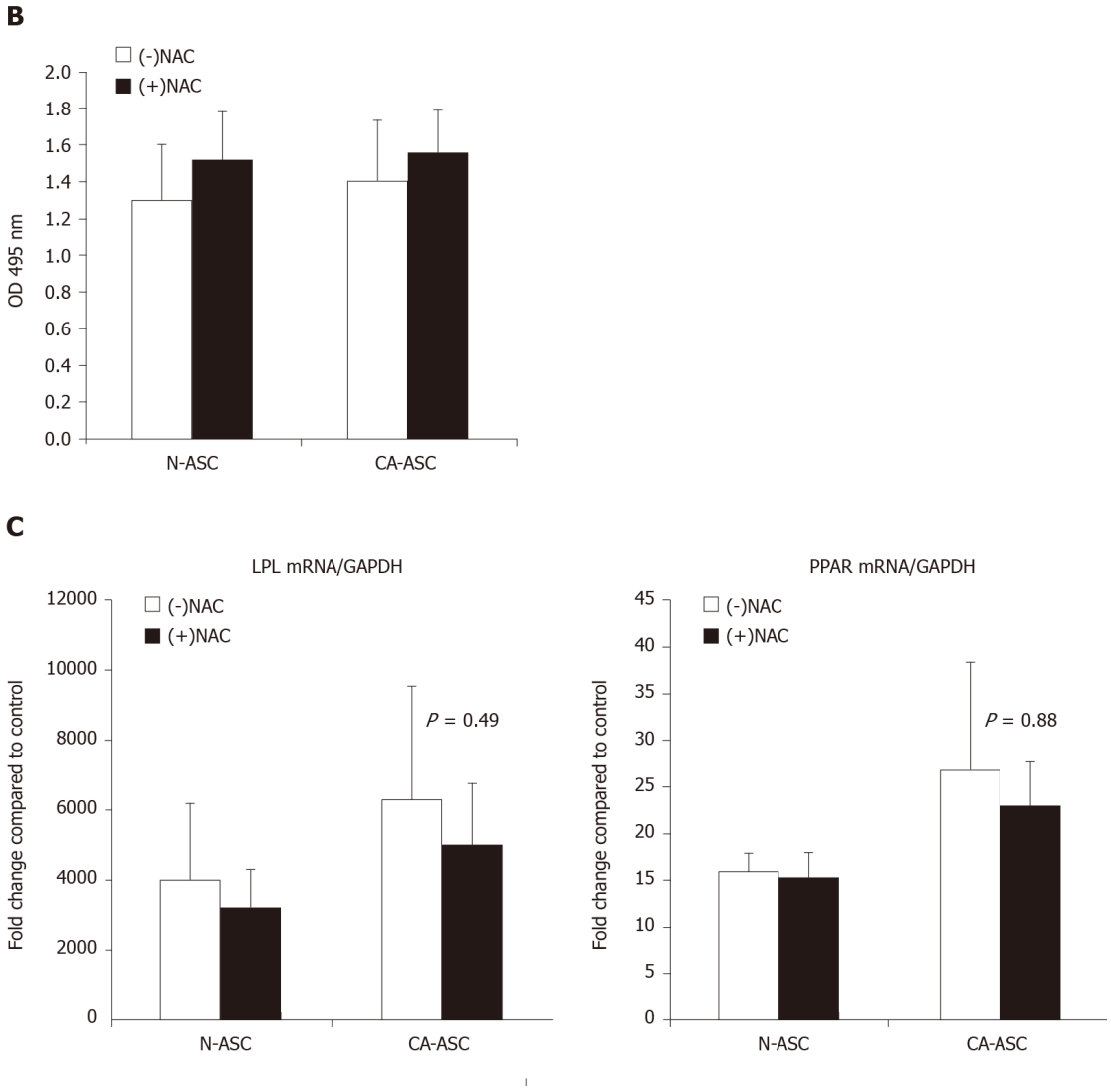


Figure 4 Adipogenic differentiation capacity of adipose-derived stromal cells in patients after received neoadjuvant chemotherapy treatment. A: Oil red O stains in the adipogenic-induced ASCs from the cancerous side of the breast (CA-ASC) and noncancerous side of the breast (N-ASC) in patients receiving NAC treatment (+NAC) *vs* not-receiving NAC (-NAC) from undifferentiated ASCs (left) and differentiated ASCs (right). B: Quantified by extracting the dyes for evaluating the adipogenic differentiated cells levels from the cancerous side of the breast or noncancerous side of the breast ASCs in patients receiving NAC treatment *vs* not-receiving NAC. C: Real-time PCR evaluating the mRNA expression of peroxisome proliferator activated receptor gamma (PPARγ) and lipoprotein lipase (LPL) in differentiating ASCs from the cancerous side of the breast or noncancerous side of the breast in patients receiving NAC treatment *vs* not-receiving NAC (n = 21, mean ± SE, P = NS). ASC: Adipose-derived stromal cell; NAC: Neoadjuvant chemotherapy.

commitment toward an adipocyte lineage upon *in vitro* cultured in derivative-specific differentiation medium. This finding is important; the use of harvested autologous stem cells back to the treating surgeon is likely to be necessary for the maintenance of cell function before implantation. Another important point, the ASCs yield and proliferation rates of ASCs from the cancerous side of the breast was showed lower than the ASCs that from the noncancerous side of the breast in both patients receiving NAC and not-receiving NAC. However, the ability of ASCs to differentiate toward an adipocyte lineage from the cancerous side of the breast was showed similar to those ASCs that obtained from the noncancerous side of the breast suggested that the chemotherapy does not significantly alter the ability of adipocyte characteristics acquired by the stem cells in the tumor environment. To our knowledge, this is the first direct demonstration showing that ASCs from the cancerous side of the breast were capable of surviving at their differentiation potential in patients receiving the cancer treatment. Nevertheless, evaluation of the effects of chemotherapy in breast cellular interactions between the mesenchymal stem cells/or cancer stem cells and tumor cells will require in our future study[24,25].

In addition to confirming the availability of these stem cells in a cancer population, this study provides evidence that ASCs from cancer patients after exposure to chemo-treatment can retain their proliferation and differentiation capacity to acquire several important adipocyte characteristics. The results are consistent with other *in vitro*

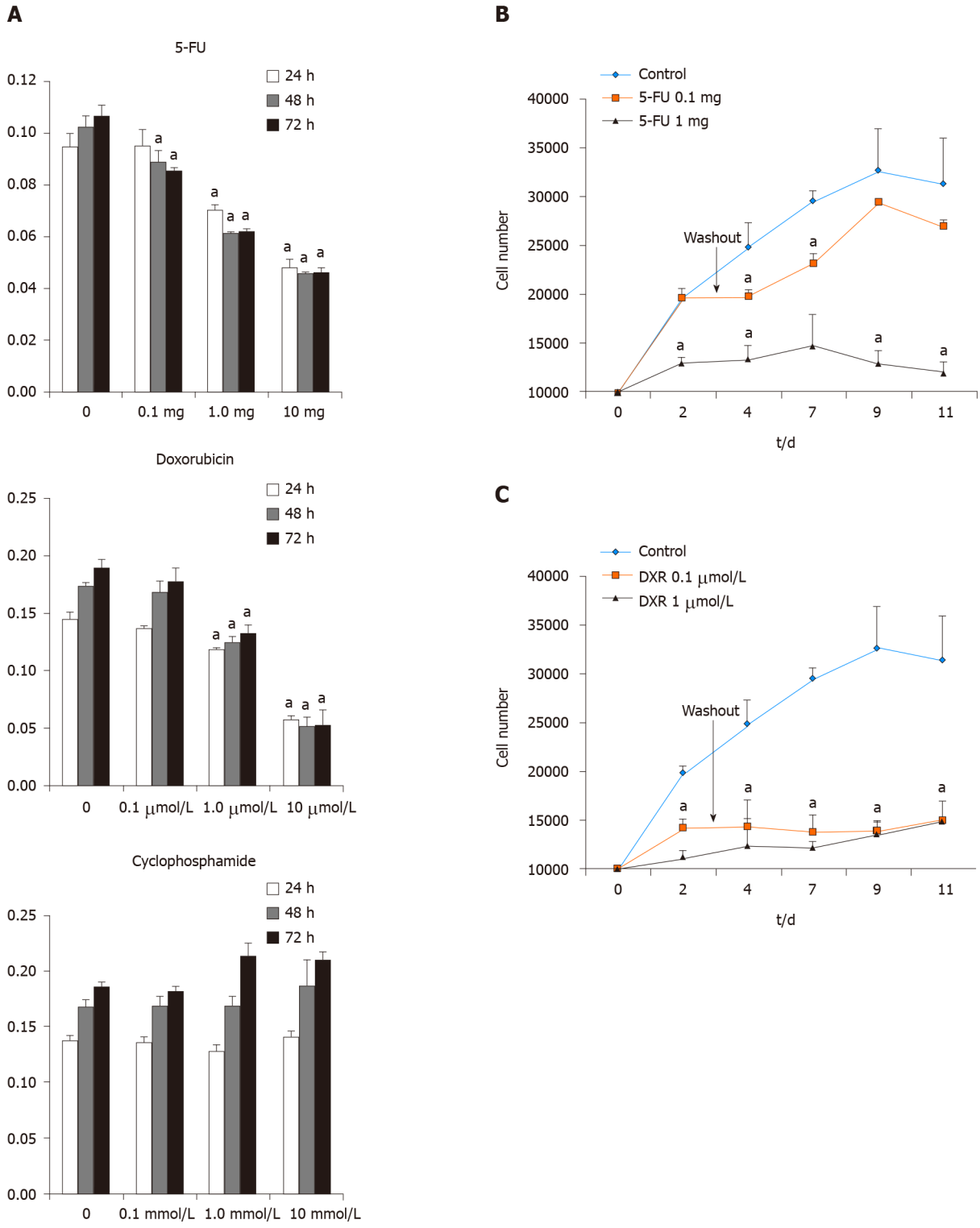


Figure 5 Recovery of adipose-derived stromal cells analysis following exposure to individual chemotherapeutic agents *in vitro* human population. A: ASCs were isolated from female patients during reconstructive procedures. Cell viability was measured by MTT assays after ASCs treated with different dosages of 5-FU, DXR and cyclophosphamide on 24, 48, and 72 h. B: Growth curves of ASCs treated with 5-FU or DXR for 72 h then removed and the cells were cultured in medium without drugs for an additional 8 d. The results represent the mean ± SE of triplicate cultures of three representative experiments. $n = 3$, $^{a}P < 0.05$ *vs* control. 5-FU: 5-fluorouracil; DXR: Doxorubicin.

studies showing that human mesenchymal stromal cells were able to maintain their multi-differentiation potential after treatment with various chemotherapeutic agents[26-28]. This may also become important; several studies have shown that grafted fat has an increased survival rate when transplanted with the adipose-derived stem cells[10,29-31].

Previous work from our lab has shown that *in vitro* direct exposure chemotherapeutic agents of paclitaxel and tamoxifen modulated human ASC cellular

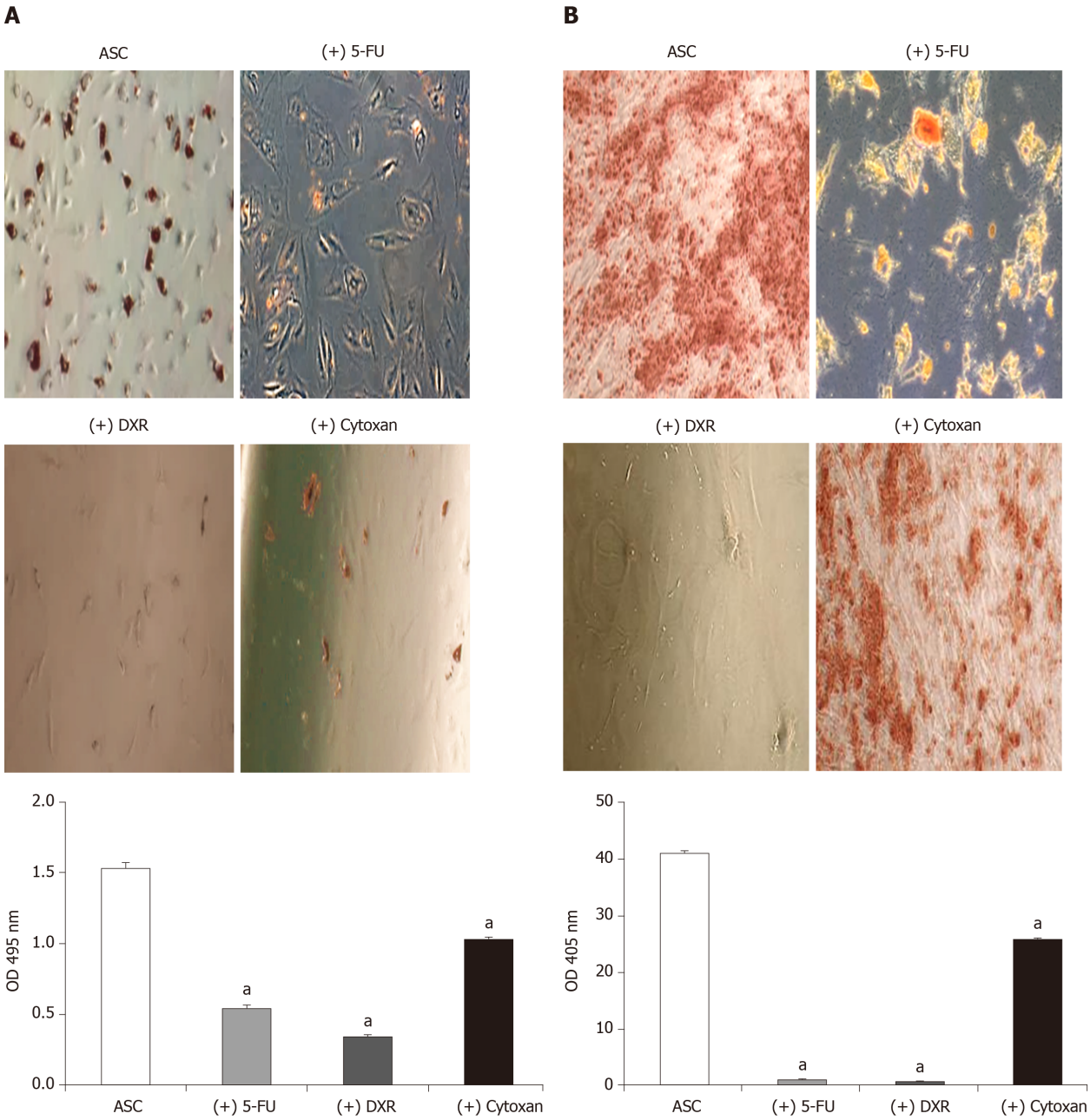


Figure 6 Differentiation capacity of adipose-derived stromal cells analysis following exposure to individual chemotherapeutic agents *in vitro* human population. A: Oil red O stains, quantified by extracting the dyes for evaluating the adipogenic differentiated cell levels. B: Alizarin red stains, quantified by extracting the dyes for evaluating the osteogenic differentiated cell levels. ASCs were isolated from female patients during reconstructive procedures. n = 3, mean ± SE, ^{a}P < 0.05 *vs* control. ASC: Adipose-derived stromal cell; 5-FU: 5-fluorouracil; DXR: Doxorubicin; OD: Optical density.

functions[13-15]. In the present study, we evaluated the recovery of ASC cellular functions after exposure to another three clinically useful chemotherapeutic agents of 5-FU, DXR and cyclophosphamide by using *in vitro* culture system. The predominant neoadjuvant chemotherapeutics for breast cancer are Taxol's, doxorubicin, cyclophosphamide, and 5-fluoruracil, and there remains limited research describing how these drugs affects stem cells function[32]. In our study, we found that after cessation and washout of the drugs for a week, ASCs showed recovery of the cell growth capacity in lower doses of 5-FU treated groups which compared to the higher doses of 5-FU treated groups. However, the recovery of cell viability was not seen in ASCs treated with higher doses of 5-FU groups and doxorubicin treated groups, after the withdrawal of the drugs respectively. As this time-lapse is considerably longer than the 8 d withdrawal period examined in our *in vitro* setting, the ASCs likely recovered from the cytotoxic effects of their therapy with additional time. Further studies are needed to investigate the timeframe of ASC functional recovery after treated with chemotherapeutic drugs. Additionally, in our study, we have observed that cyclophosphamide did not inhibit ASCs growth. This correlates with previous

studies and provides that not all chemotherapeutic agents affect the viability of stem cells[33]. Moreover, a study by Beane *et al*[33] demonstrated that the growth of ASCs was inhibited by clinically relevant concentrations of vincristine, cytarabine, and etoposide, but these cells contrarily appeared resistant to high-dose methotrexate treatment.

There are only a few *in vitro* studies showing human mesenchymal stem cell (bone marrow or ASC) characteristics in the presence of chemotherapeutic drugs and radiation[7,13-15,23]. Unfortunately, no human studies are evaluating the recovery of ASC differentiation capabilities in patients receiving neoadjuvant chemotherapy. Therefore, to the best of our knowledge, our results are the first time in which a human study directly demonstrates that ASCs have the potential to recover differentiation capacity in patients after receiving chemotherapy. We would note that by observing the *in vitro* culture system direct exposure chemotherapeutic agents to human ASCs and in patients with receiving the chemotherapy treatment, our results indicated that despite the *in vitro* evidence of the negative effects of chemotherapeutic agents on the ASCs, it might not be clinically relevant as *ex vivo* examination of patient's ASC shows these cells can functionally recover after various neoadjuvant chemotherapy regimens. Our data may well provide new information to better understand the use of autologous ASCs for fat grafting and reconstruction in breast cancer patients undergoing treatment.

These are several limitations to this study, including the relatively small numbers of patients and the comparison of ASCs before posting the chemotherapy and after cessation of NAC treatment. Therefore, determine the temporal effects of chemotherapy before, during chemo-treatment and after cessation to evaluate the ASCs function recovery potential in patients will be required in our future studies. In addition, at this time, the limited tissue samples that could be obtained from the patients limited the number of studies we could perform. We were only able to look at the adipogenic differentiation of ASCs in the *ex vivo* study and unable to look at the osteogenic or endothelial differentiation and their stem cell characteristics. Furthermore, this was a pilot study consisting of only 21 patients; a larger randomized study of *ex vivo* samples is needed to confirm our findings that neoadjuvant chemotherapy does not affect the ASCs functions. We did not take into account the different variations of neoadjuvant chemotherapy regimens the patients received due to the small sample size. However, all of the patients who did receive neoadjuvant chemotherapy did receive Taxol and completed therapy about 4-6 wk prior to the isolation of ASCs.

In conclusion, this study provides new and novel insight information regarding the use of autologous mesenchymal stem cells derived from adipose tissue in cancer patients after exposure to chemotherapy, namely, (1) the availability of these cells for use does not appear to be adversely affected by post-chemotherapy (in fact, the yield of ASCs didn't alter much after NAC treatment of patients); (2) the proliferation rates of ASCs derived from patients didn't differ much before and after NAC upon *in vitro* culture; and (3) these cells can appear to retain the differentiation capacity to acquire adipocyte traits simile to those ASCs that obtained from the patients not-receiving NAC. Further, we evaluated the cellular function recovery of ASCs after exposure to three clinically useful chemotherapeutic agents. The study of our results indicated that despite the *in vitro* evidence of the negative effects of chemotherapeutic agents on the ASCs, it might not be clinically relevant as *ex vivo* examination shows these cells from patients can functionally recover after various neoadjuvant chemotherapy regimens. Overall, the present study is the first report that the breast adipose tissue appears to will be a viable source of autologous stem cells and ASCs may hold great potential and represents to serve as a cell source for use in fat grafting and reconstruction in cancer patients undergoing chemotherapy.

ARTICLE HIGHLIGHTS

Research background

In cancer patients, post-exposure to radiation and chemotherapy suggests that these cancer treatment therapies may limit stem cells cellular functions important for soft tissue wound healing. For clinical translation to patients that have undergone cancer treatment, it is necessary to understand the effects of these therapies on the adipose-derived stromal/stem cell (ASC)'s ability to improve fat graft survival in clinical practice. Herein, we examined the effects of chemotherapy on ASCs outcomes in patients with receiving neoadjuvant therapies and compared to the patients not-receiving neoadjuvant chemotherapy (NAC) treatment.

Research motivation

Recent research has focused almost entirely on poor soft tissue wound healing in patients exposure to radiation/or chemotherapy, but little is known about the recovery of cell viability

and function capability of stem cells in patients receiving chemotherapeutic-treatment. This research focused on characteristics of stem cells isolated from human adipose tissue: (1) The cellular function of ASCs diminished in direct exposure to chemotherapeutic agents, and potency to recovery after cessation of these drugs in treatment; and (2) Availability in receiving NAC treatment of population most likely the ASCs may hold great potential to serve as a cell source for fat grafting and reconstruction in cancer patients undergoing chemo-treatment. This research will provide new and novel insight information regarding the use of autologous mesenchymal stem cells derived from adipose tissue in cancer patients after exposure to chemotherapy.

Research objectives

The main objective of this study was to investigate whether the impact on ASCs function capacity and recovery in cancer patients may be due to the chemotherapy. In addition, we evaluated in vitro, whether ASCs have the potential for recovery of cellular function after exposure to three commonly utilized clinical chemotherapeutic agents.

Research methods

We analyzed the stem cells yield, proliferation rates, and adipogenesis differentiation capacity of ASCs from breast cancer patients with receiving NAC treatment or not-receiving NAC. We also measured the recovery of the cellular functions of ASCs after treated with three chemotherapeutic agents by *in vitro* culture system.

Research results

We reveal that the yield of ASCs didn't alter much after NAC treatment of patients. The proliferation rates of ASCs derived from patients didn't differ much before and after NAC upon *in vitro* culture, and these cells appeared to retain the capacity to acquire adipocyte traits simile to the ASCs that from patients not-receiving NAC. By observing the *in vitro* culture system, the study indicates that the full recovery of cell proliferation rates was not observed in ASCs after the withdrawal of drug treatment in a short time interval.

Research conclusions

We conclude that (1) the availability of ASCs for use does not appear to be adversely affected by post-chemotherapy; (2) despite the *in vitro* evidence of the negative effects of chemotherapeutic agents on the ASCs, it might not be clinically relevant as *ex vivo* examination of patient's ASC shows these cells can functionally recover after various neoadjuvant chemotherapy regimens; and (3) the breast adipose tissue appears to will be a viable source of autologous stem cells and ASCs may hold great potential and represents to serve as a cell source for use in fat grafting and reconstruction in patients undergoing chemotherapy such as in breast cancer patients.

Research perspectives

The study of our results provides novel insight into the use of autologous stem cell-based target therapy in reconstructive procedures in cancer patients that have received chemotherapy. Further study is needed to determine the temporal effects of chemotherapy before, during chemo-treatment and after cessation to evaluate ASC function and recovery potential in patients to clarify whether the impact on ASC function and recovery components may be due to the chemotherapy.

REFERENCES

1 **Ferlay J**, Soerjomataram I, Dikshit R, Eser S, Mathers C, Rebelo M, Parkin DM, Forman D, Bray F. Cancer incidence and mortality worldwide: sources, methods and major patterns in GLOBOCAN 2012. *Int J Cancer* 2015; **136**: E359-E386 [PMID: 25220842 DOI: 10.1002/ijc.29210]

2 **Malhaire C**, Hequet D, Falcou MC, Feron JG, Tardivon A, Leduey A, Guillot E, Mosseri V, Rouzier R, Couturaud B, Reyal F. Outcome of oncoplastic breast-conserving surgery following bracketing wire localization for large breast cancer. *Breast* 2015; **24**: 370-375 [PMID: 25913288 DOI: 10.1016/j.breast.2015.02.037]

3 **Surgeons ASoP**. Report of the 2010 plastic surgery statistics: ASPS national clearinghouse of plastic surgery procedural statistics. Available from: www.plasticsurgery.org

4 **Schmauss D**, Machens HG, Harder Y. Breast Reconstruction after Mastectomy. *Front Surg* 2015; **2**: 71 [PMID: 26835456 DOI: 10.3389/fsurg.2015.00071]

5 **Coleman SR**. Structural fat grafting: more than a permanent filler. *Plast Reconstr Surg* 2006; **118**: 108S-120S [PMID: 16936550 DOI: 10.1097/01.prs.0000234610.81672.e7]

6 **Pearl RA**, Leedham SJ, Pacifico MD. The safety of autologous fat transfer in breast cancer: lessons from stem cell biology. *J Plast Reconstr Aesthet Surg* 2012; **65**: 283-288 [PMID: 21820375 DOI: 10.1016/j.bjps.2011.07.017]

7 **Toyserkani NM**, Quaade ML, Sørensen JA. Cell-Assisted Lipotransfer: A Systematic Review of Its Efficacy. *Aesthetic Plast Surg* 2016; **40**: 309-318 [PMID: 26893280 DOI: 10.1007/s00266-016-0613-1]

8 **Fu S**, Luan J, Xin M, Wang Q, Xiao R, Gao Y. Fate of adipose-derived stromal vascular fraction cells after co-implantation with fat grafts: evidence of cell survival and differentiation in ischemic adipose tissue. *Plast Reconstr Surg* 2013; **132**: 363-373 [PMID: 23897335 DOI: 10.1097/PRS.0b013e31829588b3]

9 **Mizuno H**, Tobita M, Uysal AC. Concise review: Adipose-derived stem cells as a novel tool for future regenerative medicine. *Stem Cells* 2012; **30**: 804-810 [PMID: 22415904 DOI: 10.1002/stem.1076]

10 **Zhu M**, Zhou Z, Chen Y, Schreiber R, Ransom JT, Fraser JK, Hedrick MH, Pinkernell K, Kuo HC. Supplementation of fat grafts with adipose-derived regenerative cells improves long-term graft retention. *Ann Plast Surg* 2010; **64**: 222-228 [PMID: 20098110 DOI: 10.1097/SAP.0b013e31819ae05c]

11 **Mitchem J**, Herrmann D, Margenthaler JA, Aft RL. Impact of neoadjuvant chemotherapy on rate of tissue expander/implant loss and progression to successful breast reconstruction following mastectomy. *Am J Surg* 2008; **196**: 519-522 [PMID: 18809054 DOI: 10.1016/j.amjsurg.2008.06.016]

12 **Zweegman S**, Kessler FL, Kerkhoven RM, Heimerikx M, Celie JW, Janssen JJ, Huijgens PC, Drager AM, van den Born J. Reduced supportive capacity of bone marrow stroma upon chemotherapy is mediated via changes in glycosaminoglycan profile. *Matrix Biol* 2007; **26**: 561-571 [PMID: 17521897 DOI: 10.1016/j.matbio.2007.04.006]

13 **Pike S**, Zhang P, Wei Z, Wu N, Klinger A, Chang S, Jones R, Carpenter J, Brown SA, DiMuzio P, Tulenko T, Liu Y. In vitro effects of tamoxifen on adipose-derived stem cells. *Wound Repair Regen* 2015; **23**: 728-736 [PMID: 26043659 DOI: 10.1111/wrr.12322]

14 **Choron RL**, Chang S, Khan S, Villalobos MA, Zhang P, Carpenter JP, Tulenko TN, Liu Y. Paclitaxel impairs adipose stem cell proliferation and differentiation. *J Surg Res* 2015; **196**: 404-415 [PMID: 25891676 DOI: 10.1016/j.jss.2015.03.026]

15 **Harris WM**, Zhang P, Plastini M, Ortiz T, Kappy N, Benites J, Alexeev E, Chang S, Brockunier R, Carpenter JP, Brown SA. Evaluation of function and recovery of adipose-derived stem cells after exposure to paclitaxel. *Cytotherapy* 2017; **19**: 211-221 [PMID: 27887867 DOI: 10.1016/j.jcyt.2016.10.010]

16 **Dominici M**, Rasini V, Bussolari R, Chen X, Hofmann TJ, Spano C, Bernabei D, Veronesi E, Bertoni F, Paolucci P, Conte P, Horwitz EM. Restoration and reversible expansion of the osteoblastic hematopoietic stem cell niche after marrow radioablation. *Blood* 2009; **114**: 2333-2343 [PMID: 19433859 DOI: 10.1182/blood-2008-10-183459]

17 **Kronowitz SJ**, Mandujano CC, Liu J, Kuerer HM, Smith B, Garvey P, Jagsi R, Hsu L, Hanson S, Valero V. Lipofilling of the Breast Does Not Increase the Risk of Recurrence of Breast Cancer: A Matched Controlled Study. *Plast Reconstr Surg* 2016; **137**: 385-393 [PMID: 26818270 DOI: 10.1097/01.prs.0000475741.32563.50]

18 **Charvet HJ**, Orbay H, Wong MS, Sahar DE. The Oncologic Safety of Breast Fat Grafting and Contradictions Between Basic Science and Clinical Studies: A Systematic Review of the Recent Literature. *Ann Plast Surg* 2015; **75**: 471-479 [PMID: 26360655 DOI: 10.1097/SAP.0000000000000604]

19 **Oh E**, Chim H, Soltanian HT. The effects of neoadjuvant and adjuvant chemotherapy on the surgical outcomes of breast reconstruction. *J Plast Reconstr Aesthet Surg* 2012; **65**: e267-e280 [PMID: 22633392 DOI: 10.1016/j.bjps.2012.04.053]

20 **Holmes D**, Colfry A, Czerniecki B, Dickson-Witmer D, Francisco Espinel C, Feldman E, Gallagher K, Greenup R, Herrmann V, Kuerer H, Malik M, Manahan E, O'Neill J, Patel M, Sebastian M, Wheeler A, Kass R. Performance and Practice Guideline for the Use of Neoadjuvant Systemic Therapy in the Management of Breast Cancer. *Ann Surg Oncol* 2015; **22**: 3184-3190 [PMID: 26224406 DOI: 10.1245/s10434-015-4753-3]

21 Breast Cancer Version 2. Plymouth Meeting, PA: National Comprehensive Cancer Network, 2016. Available from: www.NCCN.org

22 **Zhang P**, Moudgill N, Hager E, Tarola N, Dimatteo C, McIlhenny S, Tulenko T, DiMuzio PJ. Endothelial differentiation of adipose-derived stem cells from elderly patients with cardiovascular disease. *Stem Cells Dev* 2011; **20**: 977-988 [PMID: 20879833 DOI: 10.1089/scd.2010.0152]

23 **Gentile P**, Casella D, Palma E, Calabrese C. Engineered Fat Graft Enhanced with Adipose-Derived Stromal Vascular Fraction Cells for Regenerative Medicine: Clinical, Histological and Instrumental Evaluation in Breast Reconstruction. *J Clin Med* 2019; **8** [PMID: 31013744 DOI: 10.3390/jcm8040504]

24 **Chulpanova DS**, Kitaeva KV, Tazetdinova LG, James V, Rizvanov AA, Solovyeva VV. Application of Mesenchymal Stem Cells for Therapeutic Agent Delivery in Anti-tumor Treatment. *Front Pharmacol* 2018; **9**: 259 [PMID: 29615915 DOI: 10.3389/fphar.2018.00259]

25 **Kusuma GD**, Carthew J, Lim R, Frith JE. Effect of the Microenvironment on Mesenchymal Stem Cell Paracrine Signaling: Opportunities to Engineer the Therapeutic Effect. *Stem Cells Dev* 2017; **26**: 617-631 [PMID: 28186467 DOI: 10.1089/scd.2016.0349]

26 **Li J**, Law HK, Lau YL, Chan GC. Differential damage and recovery of human mesenchymal stem cells after exposure to chemotherapeutic agents. *Br J Haematol* 2004; **127**: 326-334 [PMID: 15491295 DOI: 10.1111/j.1365-2141.2004.05200.x]

27 **Liang W**, Xia H, Li J, Zhao RC. Human adipose tissue derived mesenchymal stem cells are resistant to several chemotherapeutic agents. *Cytotechnology* 2011; **63**: 523-530 [PMID: 21761127 DOI: 10.1007/s10616-011-9374-5]

28 **Mueller LP**, Luetzkendorf J, Mueller T, Reichelt K, Simon H, Schmoll HJ. Presence of mesenchymal stem cells in human bone marrow after exposure to chemotherapy: evidence of resistance to apoptosis induction. *Stem Cells* 2006; **24**: 2753-2765 [PMID: 16931776 DOI: 10.1634/stemcells.2006-0108]

29 **Lopatina T**, Kalinina N, Karagyaur M, Stambolsky D, Rubina K, Revischin A, Pavlova G, Parfyonova Y, Tkachuk V. Adipose-derived stem cells stimulate regeneration of peripheral nerves: BDNF secreted by these cells promotes nerve healing and axon growth de novo. *PLoS One* 2011; **6**: e17899 [PMID: 21423756 DOI: 10.1371/journal.pone.0017899]

30 **Piccinno MS**, Veronesi E, Loschi P, Pignatti M, Murgia A, Grisendi G, Castelli I, Bernabei D, Candini O, Conte P, Paolucci P, Horwitz EM, De Santis G, Iughetti L, Dominici M. Adipose stromal/stem cells assist fat transplantation reducing necrosis and increasing graft performance. *Apoptosis* 2013; **18**: 1274-1289 [PMID: 23828239 DOI: 10.1007/s10495-013-0878-7]

31 **Harris WM**, Plastini M, Kappy N, Ortiz T, Chang S, Brown S, Carpenter JP, Zhang P. Endothelial Differentiated Adipose-Derived Stem Cells Improvement of Survival and Neovascularization in Fat Transplantation. *Aesthet Surg J* 2019; **39**: 220-232 [PMID: 29846494 DOI: 10.1093/asj/sjy130]

32 **Beane OS**, Fonseca VC, Darling EM. Adipose-derived stem cells retain their regenerative potential after methotrexate treatment. *Exp Cell Res* 2014; **327**: 222-233 [PMID: 24992046 DOI: 10.1016/j.yexcr.2014.06.015]

33 **Taylor CW**, Horgan K, Dodwell D. Oncological aspects of breast reconstruction. *Breast* 2005; **14**: 118-130 [PMID: 15767181 DOI: 10.1016/j.breast.2004.08.006]

Published By Baishideng Publishing Group Inc
7041 Koll Center Parkway, Suite 160, Pleasanton, CA 94566, USA
Telephone: +1-925-3991568
E-mail: bpgoffice@wjgnet.com
Help Desk: https://www.f6publishing.com/helpdesk
https://www.wjgnet.com

© 2020 Baishideng Publishing Group Inc. All rights reserved.